UNIVERSITA' DEGLI STUDI DI NAPOLI
"FEDERICO II"

Dottorato di Ricerca in "Scienze Biomorfologiche e Chirurgiche"

XXXII Cycle

Identification of new molecular markers of thyroid cancer progression

Tutor: Prof.ssa Giuliana Salvatore **Ph.D. student Paola Lucia Chiara Iervolino**

Coordinator: Prof. Alberto Cuocolo

Academic Year: 2019/2020

INTRODUCTION

RESULTS (I)

RESULTS (II)

1. Thyroid cancer

Thyroid cancer is a common type of endocrine malignancy and its incidence in the last 50 years is increasing significantly and it is project to become the fourth leading type of tumor in the world (Kim *et al*.; 2020). The substantial increase of this disorder is likely associated to an increased use of imaging techniques, biopsy procedures and proactive screening programs (Bible *et al*.; 2016).

Different risk factors for thyroid cancer have been identified, such as patients' age, sex, ethnicity and family history of thyroid cancer, exposure to ionizing radiation and obesity. Another important factor that can contribute to the increasing incidence of thyroid cancer is cigarette smoking that can reduces levels of thyroid hormones and estrogens and decreases the prevalence of serum thyroid autoantibodies (Kitahara *et al*.; 2016).

There are several histological types and subtypes of thyroid cancer with different cellular origins, characteristics and prognoses. Thyroid cancers can derive from two type of thyroid cells: follicular cells and parafollicular C cells.

Thyroid tumors that origins from follicular cells are classified in specific cancer subtypes including:

- **Well-differentiated thyroid cancer** (WDTC), that is the most frequent neoplasm of the endocrine system (more than 95% of cases) with a favorable prognosis and generally cured by surgery and radio-iodine (Cabanillas *et al*.; 2016). WDTC are represented by papillary thyroid carcinoma (PTC, ~85% of the cases) **(**Siegel *et al*.; 2017; Durante *et al*.; 2018**)**, follicular thyroid carcinoma (FTC, ~15%), (Fagin *et al*.; 2016) and hurthle cell thyroid cancer (HCC). HCC has a frequency of ~3% to 5% of all types of thyroid cancer, according to the World Health Organization (WHO) (DeLellis *et al*.; 2004).
- **Poorly differentiated thyroid cancer** (PDTC) represents ~5% of cases, both morphologically and prognostically, occupy an intermediate position between differentiated (follicular and papillary) and undifferentiated thyroid carcinomas (Patel *et al*.; 2014).

- **Anaplastic thyroid cancer (undifferentiated)** (ATC) constitutes less than 5% of thyroid malignancies with a mortality rate that is over 90% and a mean survival time of ~3-6 months after the diagnosis. ATC is defined by the WHO as a highly malignant tumor completely or partially composed of undifferentiated cells (Smallridge *et al.*; 2012).

PDTC and ATC can develop *de novo* or derive from differentiated thyroid cancer (Cabanillas *et al.;* 2016).

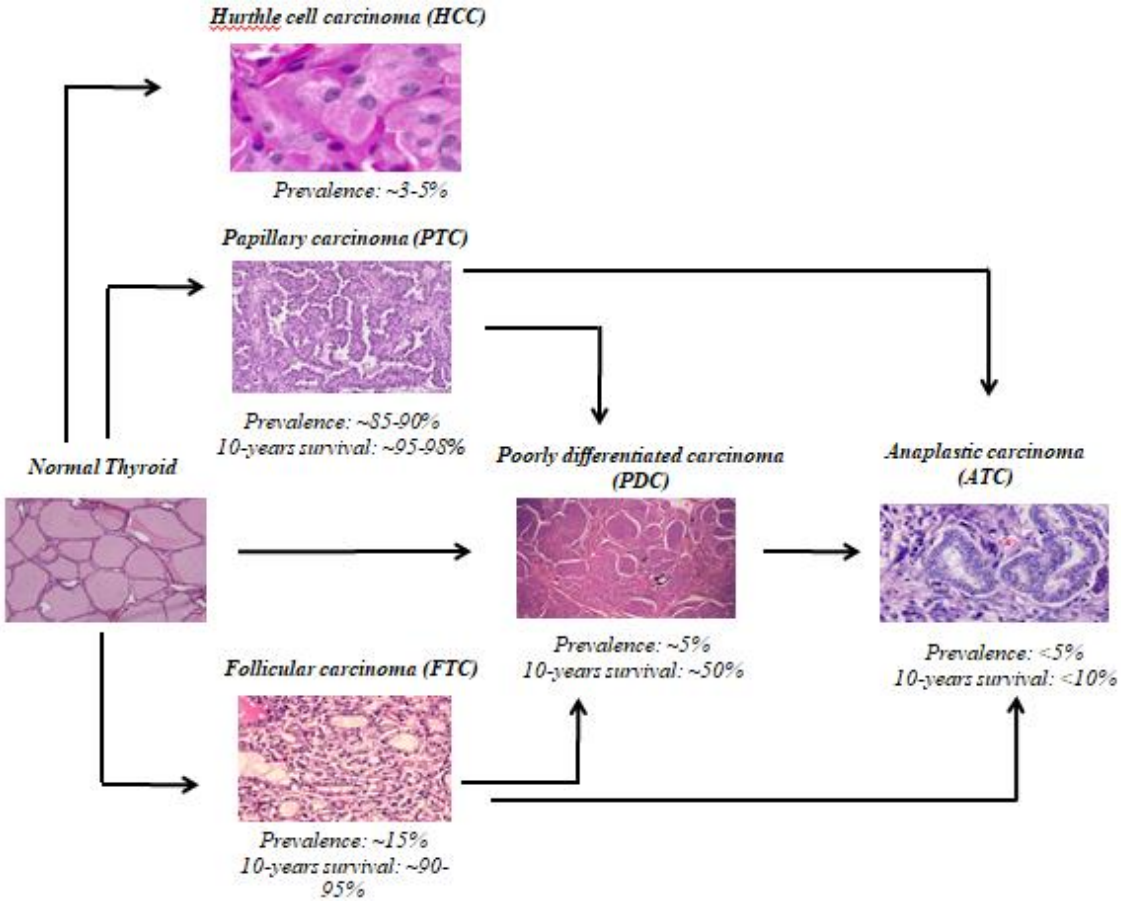

Figure 1. Classification of thyroid carcinogenesis. Scheme of dedifferentiation of follicular cell-derived thyroid carcinoma with main histological features

Parafollicular C cell-derived medullary thyroid cancer (MTC) represents ~ 3-5% of thyroid malignancies, is a neuroendocrine tumor and is generally sporadic, only 20-30% of MTC cases are familial (Ceolin *et al*.; 2019).

1.1 Morphological and clinical features of follicular cell derived thyroid cancer

Papillary thyroid carcinoma (PTC) is the most frequent type of thyroid cancer (~85-90% of cases) whose incidence is on the rise. PTC can occur at any age, the mean age is about 40 years, and they are more frequent in the women respect to men. They are typically characterized by a favorable prognosis with less than 2% mortality at 5 years and are cured by surgery and radiotherapy (RAI) (Kitahara *et al*.; 2019). Histological features of PTC are papillary structures with a central fibrovascular axis and typical nuclear modifications known as "ground glass", pseudo inclusions and nuclear measurements.There are other different PTC variants that are particularly aggressive and associated with higher tumor stages and lymph-node metastases at diagnosis. These variants are the tall cell classical variant, columnar, hobnail and solid variants (Filetti *et al*.; 2019)

Follicular thyroid carcinoma (FTC) represents ~ 10 to 15% of all thyroid cancer (*Fagin et al., 2016*). FTCs are defined by the World Health Organization as malignant epithelial tumors, and histologically has three subtypes: minimally invasive FTC (encapsulated and with invasion only of the capsule); encapsulated angioinvasive FTC and widely invasive FTC (Fugazzola *et al*.; 2019). The prognosis of patients with these cancers depends of different factors such as age of patients, size and subtype of tumor (James *et al*.; 2016).

Hurtle cell thyroid carcinoma (HCC) is characterized by an aggressive growth and it is associated with a higher rate of distant metastases. Hurtle cells carcinoma presents chromosomal losses and mitochondrial DNA mutation. HCC cells are large, polygonal with high eosinophilic and granular cytoplasm. HCC, histologically, is subdivided into 2 groups: minimally invasive or widely invasive. Minimally invasive carcinomas are encapsulated tumors with capsular or vascular invasion, while,

widely invasive tumors have extensive vascular invasion and extrathyroidal invasion (Montone *et al*.; 2008).

Poorly differentiated thyroid carcinoma (PDTC) is a follicular thyroid neoplasm. They are characterized by a solid-trabecular-insular pattern of growth, high mitotic rate and tumor necrosis. In PDTC are frequent vascular invasion, distant metastases. These carcinomas have also a poor response to radioiodine therapy and have a 5-year overall survival rate of ~60–85% (Fugazzola *et al*.; 2019).

Anaplastic thyroid carcinoma (ATC) has an incidence of ~ 1.7% and mortality rate of ~ 33%–50% (Jayarangaiah *et al*.; 2019). It represents the most rare and aggressive form of human cancer with poor prognosis and a mean survival time of 4 months after the diagnosis (Pozdeyev *et al*.; 2020). ATC is unresponsive to radioactive iodine treatment and is characterized by rapid tumor growth, local invasion and high rate of distant metastasis. Indeed, ATC is associated with a high morbidity and mortality; most of the patients are classified as stage IV at the moment of diagnosis (Tiedje *et al*.; 2018). In the recent years, the identification of new molecular determinants of ATC, have led to several clinical trials for development of new target therapies.

1.2 Genetic alterations in papillary thyroid carcinoma

Thyroid tumorigenesis and progression are associated to different driver mutations of the mitogen-activated protein kinase (MAPK) and phosphoinositide 3-kinase (PI3K) signaling pathways. In particular, in PTC, common genetic alterations include point mutations in the BRAF (~62%) and RAS genes (~13%), and chromosomal rearrangements of the RET proto-oncogene (~7%). Uncommon molecular alterations in PTC are NTRK3 fusion in ~1.5%, NTRK1 fusion in ~1.3%, and TERT promoter in ~9% of cases.

Studies have shown that there is a correlation between the oncogenic genotype and histopathology phenotype of thyroid cancer (Haroon *et al*.; 2019).

BRAF is a human gene that encodes a serine/threonine protein kinase B-RAF (Li *et al.*; 2015; Fagin *et al*.; 2016). BRAF can be activated by point mutations, small in-frame deletions or insertions or by chromosomal rearrangement. The most common oncogenic mutation in BRAF is thymine to adenine transversion at position 1799 (T1799A) resulting in the substitution of valine by glutamate at residue 600 (V600E). This mutation causes constitutive activation of BRAF kinase and uncontrolled activity of the MAPK signaling pathway. This mutation is detected in ~ 60% of all PTCs. BRAF-V600E mutation is associated with highly aggressive clinical-pathological features of thyroid cancer such as the presence of distant metastases, local invasion, low expression of thyroid differentiation marker, recurrence and loss of the ability to capture radioactive iodine (Luzón-Toro *et al*.; 2019).

RET proto-oncogene, was identified in 1985, it is located on chromosome 10q11.2 (Takahashi *et al*.; 1985). It encodes a tyrosine kinase transmembrane receptor implicated in the signaling pathway of the glial derived neurotrophic factor family (Mulligan *et al*.; 2014).

In PTC, RET rearrangement derived from genetic recombination between the tyrosine kinase domain of the RET gene located on the 3' and 5'terminal of various partner genes (Santoro *et al*.; 1994). There are more of than 10 types of RET–PTC rearrangements, the main are RET/PTC1 and RET/PTC3, accounting for more than 90% of all the rearrangement. The partner genes for RET/PTC1 and RET/PTC3 are the coiled-coil domains containing gene 6 (CCDC6, also known as H4) and the nuclear receptor co-activator gene 4 (NcoA4, also known as ELE1) respectively. RET-PTC rearrangement cause constitutive tyrosine kinase activity of RET and these mutations are particularly frequent in classical PTC and in follicular variant PTC (Xing M *et al*.; 2013). To date, the frequency of these mutations in the PTC patients are ~10-20%. Increase levels of RET fusion protein are associated with an aggressive phenotype as regional invasion and lymph-node metastasis (Luzón-Toro *et al*.; 2019).

The RAS genes (HRAS, NRAS and KRAS) includes a family of GTP binding proteins that are involved in the activation of the MAPK and PI3K pathway signaling and regulated cell differentiation, proliferation and survival. The most common RAS mutation was found in codon 61

of NRAS followed by KRAS. Other mutations have been identified in codons 11 and 13 of RAS genes (Abdullah et al.; 2019).

Single nucleotide changes in the promoter region of TERT (C228Tand C250T) are found in ~9% of PTC. The change generates *de novo* consensus binding motifs for MAPK-dependent ETS (E-twenty-six) transcription factors (Melo *et al*.; 2015). TERT promoter mutations, together BRAF mutations are associated with high tumor aggressiveness and mortality. Other chromosomal rearrangements have been found in ~5% of PTCs, and involve the gene coding for the NTRK1 tyrosine kinase receptor of NGF (Nerve Growth Factor). This rearrangement leads to the ectopic expression of the receptor and its constitutive activation.

Recently DNA sequencing of 500 cases of PTC and genomic analysis by the Cancer Genome Atlas have confirmed the main mutations that confer a selective advantage to the thyroid cancer cell and have also identified new mutations that affect the ALK, NTRK3, MET, FGFR2, EIF1AX, THADA and the LTK genes (Cancer Genome Atlas; 2014).

Finally, a thyroid specific transcription factor, FOXE1, play an important role in thyroid progression because it regulates cellular differentiation. In PTC is also demonstrated that the loss function of this transcription factor induces an increase of different genes such as: ADAMTS9, CDH1, DUOX2 and S100A4 (Penna-Martinez *et al*.; 2014).

1.3 Genetic alterations in follicular thyroid carcinoma

FTC is characterized by RAS point mutation (~49% of cases) that affect the GTP binding domain (exon 2, codons 12 or 13) or the GTPase domain (exon 3, codon 61). This mutation leads to a loss of its function.

Another important mutation present in FTC is the PAX8/ PPARγ rearrangement (~30-58% of cases). In FTCs, PAX8–PPARγ has been associated with female gender, younger patient age, high cellularity and locally invasive features. PAX8–PPARγ positive FTCs may have a lower risk of distant metastases than tumors lacking the rearrangement.

Finally, in ~17% of FTC, TERT promoter mutation has been detected with a frequency that is higher respect to PTC. This type of mutation is associated to poor prognosis in thyroid carcinoma (Haroon *et al*.; 2019; Acquaviva *et al*.; 2018).

1.4 Genetic alterations in hurthle cell thyroid carcinoma

HCC is a thyroid tumor characterized by chromosomal losses and mitochondrial DNA mutations. In particular DNA mutations involving complex I subunits of the electron transport chain while molecular alterations associated with hürthle cell neoplasms include chromosomal rearrangement such as CHCHD10-VPREB3, HEPHL1-PANX1.and TMEM233-PRKAB1. TERT promoter mutations and TP53 mutations are common in HCC respect to PTC, indeed this type of tumor is more aggressive compared with PTC. Also, mutations in RAS and BRAF genes can occur in HCC with a low frequency (~5% and 9-15% respectively) (Gopal *et al*.; 2018; Ganly *et al.;*2018).

1.5 Genetic alterations in poorly differentiated thyroid carcinoma and anaplastic thyroid carcinoma

PDTCs have genetic features intermediate between well-differentiated and ATC. The main driver mutations in PDTC and ATC are BRAF and RAS mutation, occurring in ~ 33% and ~ 45% of PDTC and in ~ 29% and 23% of ATC respectively. Additionally, somatic mutations in the promoter of the TERT (Telomerase Reverse Transcriptase) gene have been described as highly recurrent in PDTC and ATC (40% and 73% respectively) respect to PTC and FTC (Haroon *et al*.; 2019).

For anaplastic transformation, genetic alterations in the PI3K pathway, TP53, and the TERT promoter are necessary. Activing mutations in the PIK3CA (phosphatidylinositol-4, 5-bisphosphate 3-kinase, catalytic subunit alpha) gene are also common in ATC (Charles *et al*.; 2014). Amplification of the PIK3CA genomic locus in 3q26 are mostly found in ~40% of ATC suggesting that these genetic alterations plays an important role in the progression and aggressiveness of thyroid cancer (Xing *et al*.; 2013). Importantly, the over-activation of the PI3K-AKT pathway can be induced by PTEN inactivation, including PTEN promoter methylation, deletion or point mutations that occur in ~10–20% of ATC (Nucera *et al*.; 2011). TP53 mutations have been detected in ~ 80% of ATCs, while in PDTC its frequency is ~ 10%. p53 gene encodes for a nuclear transcription factor that plays a central role in cell cycle regulation, DNA repair and apoptosis (Haddad *et al*.; 2015; Xu et al., 2016).

Anaplastic lymphoma kinase (ALK) fusions were reported infrequently in ATC. ALK is a tyrosine kinase receptor involved with the activation of both the MAPK and PI3K-AKT pathways. The most common fusion is between ALK and the Striatin (STRN) gene, which leads to constitutive activation of ALK kinase, inducing tumor formation (Kelly *et al*.; 2014). In addition, two point mutations have been identified (ALK L1198F and ALK G1201E) that result in increased tyrosine kinase activity (Murugan *et al*; 2011).

EZH2, is a histone lysine-methyl-transferase that is over-expressed in ATC. EZH2 is involved in cell proliferation and differentiation. When EZH2 is over-expressed, histone methylation is altered, silencing the PAX8 gene and leading to an aggressive phenotype. Several studies have shown that

histone deacetylation plays a role in ATC pathogenesis. Indeed, most ATC show over-expression of histone deacetylases (HDACs). Less acetylation of histones leads to an altered expression of proteins involved in the regulation of cell cycle and proliferation (Lin *et al*.; 2013).

Furthermore, PDTC and ATC are characterized by high frequency of TERT promoter mutation (~40% and ~ 73%) (Haroon *et al*.; 2019). TERT promoter mutations seem to occur prevalently in those tumors harboring mutated BRAF or RAS, suggesting that TERT alteration is acquired later during tumor development and may deliver a functional advance to BRAF or RAS driven tumors by enabling acquisition of additional genetic defects leading to disease progression (Liu *et al*.; 2014). Mutations in the CTNNB1 gene have been found in ~ 20% of ATCs. CTNNB1 gene encodes for β catenin, a cytoplasmic protein. CTNNB1 is a major component of the E-cadherin cell-cell adhesion complexes and plays an important role in the epithelial-mesenchymal transition process (Sasanakietkul *et al*.; 2017).

In PDTC and ATC have also been identified mutations in different tumor suppressor genes, such as ATM, RB1, MEN1 (~ 0%-9%). Mutations in DNA mismatch repair (MMR) genes were identified in ATC and this mutation may arise through BRAF/RAS independent mechanism indicating that this represents a novel and independent mechanism of aggressive thyroid cancer pathogenesis (Haroon *et al*.; 2019).

Kunstman *et al*, through the sequencing of 22 ATC specimens, identified other mutations in the tumor suppressors NF1 and NF2, and in the mTOR gene. Additionally, many novel genetic alterations in cell cycle genes were found in ATC. In particular, inactivating mutations in negative cell cycle regulators CDKN2A and CDKN2B and copy number gains of CCNE1 required for cell cycle G1/S transition, were highly frequent in ATC (~ 29%). These mutations are associated with the rapid growth of ATC. Moreover, mutations in genes encoding components of the SWI/SNF chromatin remodeling complex and histone modification genes are frequently seen in aggressive thyroid

carcinoma including in poorly differentiated and anaplastic thyroid cancer, proving the important role of epigenetic mechanisms in anaplastic transformation.

Finally, Pozdeyev and colleagues observed several novel mutations in ATC such as CD274 (PD-L1), PDCD1LG2 (PD-L2), and in the non-receptor tyrosine kinase JAK2 (Pozdeyev *et al.*; 2020).

In Table 1 are reported the main morphologic characteristics and the main molecular mutations in follicular cell derived thyroid cancer.

Tumor type	**Histologic characteristic**	**Main Molecular Alterations**
PTC	Papillary architecture and nuclear features that include oval shape, overlapping, inclusion and grooves.	BRAF (~ 62%) RAS (~13%)
FTC	Hypercellular and microfollicular patterns. Vascular or capsular invasion and propensity for the metastasis via the blood stream	RAS (~49%) PAX8/PPAR$_{\gamma}$ (~30%-52%) TERT promoter (~17%)
HCC	More aggressive growth and is associated with a higher rate of distant metastases. Cells are large, polygonal with high granular cytoplasm	TP53 (~7%-12%) TERT promoter (~22%-27%) RAS (~9%-15%)
PDTC	Poorly differentiated, intermediate characteristics between PTC and ATC	BRAF (~33%) RAS (~45%) TERT promoter (~40%) TP53 mutation (~59%)
ATC	Undifferentiated. Pleomorphic giant and epithelioid cells. Presence of metastases.	BRAF (~29%) RAS (~23%) TERT promoter (~73%) PIK3CA (~40%) P53 (~80%)

Table 1- Types of follicular cell derived thyroid cancer and their mutational profiles (modified from Haroon *et.al.*; 2019).

1.6 Targeted therapy for thyroid carcinomas

Most cases of differentiated thyroid cancer of follicular cell derivation are characterized by good prognosis and good response to surgery and radioactive iodine (RAI) therapy. Nevertheless, ~15% of differentiated thyroid carcinomas develop advanced disease or distant metastatic and become resistant to all therapies. The majority of patients with ATC die from aggressive local regional disease, primarily from upper airway respiratory failure. Anaplastic thyroid cancer cells lose expression of epithelial cell marker and are characterized by the absence of sodium/iodide symporter NIS.

For this reason, this type of carcinoma has a poor response to radioiodine therapy. In these patient palliative therapy is often the only option. The Food and Drug Administation (FDA) approved two multikinase inhibitor, sorafenib and lenvatinib for these tumors. Lenvatinib targets VEGFR, FGFR, PDGFR, RET and sorafenib has its effects on VEGFR, RET, and RAF (Fagin *et al*.;2016).

Vemurafenib and dabrafenib are other two selective BRAF inhibitors, that can restore RAI uptakes and efficacy, showing a partial response in 38% of patients with metastatic or unresectable (Brose *et al*.; 2016).

Another class of antineoplastic agents are histone deacetylase inhibitors that can induce cell differentiation, cell cycle arrest, and apoptosis (Smith *et al*.; 2015). Recent preclinical studies have shown the efficacy of the CDK4/6 inhibitor LEE011, known as ribociclib, in preclinical models of ATC, as well as FTC and PTC. Ribociclib was found to reduce tumor growth via suppression of the RB-E2F1 pathway (Lee *et al*.; 2018).

Therefore, an effective therapy in the treatment of thyroid tumors may be a multidisciplinary approach based on a radical surgery followed by adjuvant chemo and target therapy and external beam radiotherapy (Perri *et al*.; 2014).

AIMS OF THE STUDY

Based on the background described it seems particularly important to determine the molecular mechanism underlying thyroid cancer progression. This could led to the identification of new molecular biomarkers and target for thyroid cancer therapy.

Thus, the aim of my PhD work was to identify new molecular determinants involved in thyroid cancer progression. In particular my studies focused on two proteins: the tumor suppressor TUSC2 and the adhesion molecule JAM-A.

The specific aims were as follow:

1) Study the molecular mechanisms induced by TUSC2 in thyroid cancer cells.

2) Study the role of the JAM-A protein as a novel marker of EMT in thyroid cancer.

2. Role of TUSC2 in human carcinogenesis

The Tumor Suppressor Candidate 2 (TUSC2), also known as FUS1, as a tumor suppressor role in several human cancers.

Previous studies, conducted in my research laboratory on thyroid cancer, showed that the expression of TUSC2, evaluated by immunohistochemistry, was decreased in anaplastic thyroid sample (n = 40) compared to papillary thyroid samples (n = 20) and to normal thyroid samples (n = 37) (Orlandella *et al*.; 2016). Based on these results, during my PhD work, I studied the biological function of TUSC2 in thyroid cancer cells in order to clarify its role as novel potential biomarker for thyroid cancer and to underpin the molecular mechanisms activated in thyroid cancer cells.

TUSC2, is located in a region on chromosome 3p21.3 that is homozygously deleted in some lung and breast cancers. Loss or reduction of TUSC2 mRNA expression has been observed in ~80% of non-small cell lung cancers (NSCLCs) and in 100% of small cell lung carcinomas and this loss was attributed to 3p21.3 deletion and was associated with a poor prognosis (Prudkin *et al*.; 2008). Genes in the 3p21.3 region are associated with cell differentiation, cell proliferation, ion exchange, transportation, apoptosis, and cell death (Ji *et al*.; 2005).

Studies *in vivo* have demonstrated that overexpression of TUSC2 significantly inhibits tumor growth and progression in mouse models and that TUSC2 knockout mice show an increased frequency of spontaneous cancers (Ivanova *et al*.; 2007). Loss of TUSC2 expression at the mRNA and at protein levels was observed in various type of human tumors such as mesothelioma (Ivanova *et al*.; 2009), esophageal carcinoma (Zhang *et al*.;2013), sarcomas (Li G *et al*.; 2011) and glioblastoma (Xin *et al*. ;2015).

TUSC2 protein contains 110 amino acids and is located in mitochondria and in cytoplasm (Ivanova *et al*.; 2009). Published studies suggested that TUSC2 encodes a multifunctional protein that play an important role in many cellular processes. TUSC2 has been shown to induce G1 cell cycle arrest and apoptosis, to regulate calcium signaling because it has a binding calcium domain, to modulate the

function of different kinases such as EGFR, PDGFR, AKT and c-ABL kinases and to affect gene expression (Rimkus *et al*.; 2017).

In literature it was reported that TUSC2 expression is negatively regulated by different microRNA. The 3'untranlated region (UTR) of TUSC2 is highly conserved, strongly suggesting that it plays an important role in regulating TUSC2 expression. In particular, in lung cancer, miR-93, miR-98, and miR-197 were capable to target the 3′-UTR region of the TUSC2 and deletion of these miRNAs target sites in the TUSC2 3-′UTR rescue the expression of TUSC2 protein (Du *et al*.; 2009).

Additionally, Lee *et al*, have identified a microRNA that binds to 3′-UTR of the TUSC2 transcript and represses its translation: miR-378. They have shown that expression of miR-378 improves cell survival, reduces caspase-3 activity, and promotes tumor growth and angiogenesis in glioblastoma cells (Lee *et al*.;2007).

In Figure 2 are reported the main pathways that are regulated by TUSC2.

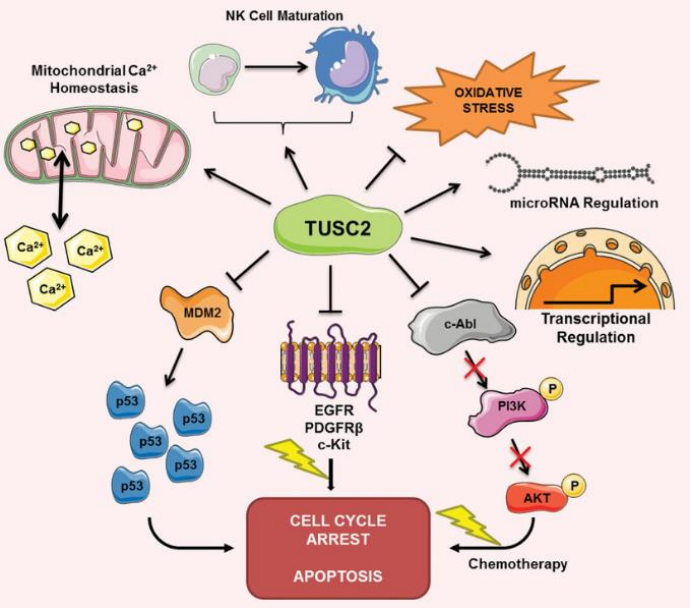

Figure 2. TUSC2 regulation of cellular processes and signaling pathways. Schematic summary of the diverse cellular processes regulated by TUSC2, including cell cycle arrest, apoptosis, calcium homoeostasis, oxidative stress response, immune response, miRNA expression, transcriptional regulation, p53/MDM pathway, and tyrosine and Ser/Thr kinases (Rimkus *et al*.; 2017).

Emerging evidence proposes that the restoration of TUSC2 expression represent an important strategy to inhibit tumor growth and tumor progression in lung cancer (Rimkus *et al*.; 2017). To translate these finding into clinical applications for molecular cancer therapy, a TUSC2 expressing nanoparticle has been developed with the aim of treating patients with lung cancer. Nanoparticles have been reported to deliver drugs and siRNA to tumors in humans. Preclinical studies in human lung cancer have demonstrated that combination treatment with TUSC2 nanovesicles and EGFR inhibitor inhibited tumor growth and metastasis (Lu *et al*.; 2012).

Studies conducted by Deng *et al.*, have demonstrated that TUSC2 restoration can potentiate the properties of cisplatin in NSCLC through downregulation of MDM2, accumulation of p53 and activation of the Apaf-1-dependent apoptosis pathway (Deng *et al*.; 2008).

Finally, since TUSC2 is capable to inhibit mTOR activation, a recent study reported that TUSC2 restoration rendered tumors more responsive to the mTOR inhibitor rapamycin in combination with erlotinib (Xiaobo *et al*.; 2016).

2.1 Role of JAM-A in human carcinogenesis

Among thyroid cancers, ATC represents the most aggressive form for which efficient therapies do not exist.

It's known that the epithelial–mesenchymal transition (EMT) represents an important mechanism involved in thyroid tumor progression and that the proteins involved in this process could represent potential novel molecular targets for treatment of these tumors.

During my PhD, I have studied the molecular mechanisms underlying the EMT process in thyroid carcinoma.

EMT is a complex process that leads, during tumorigenesis, to the loss of epithelial proprieties in polarized cells, and the acquisition of a mesenchymal phenotype that promotes tumor invasion and metastasis. This process is regulated by transcription factors that belong to SNAIL, TWIST and ZEB proteins' families that play an important role in neoplastic progression, from the first stages to tumor invasion, dissemination and metastatization (Singh *et al*.; 2017).

These transcription factors are also involved in the resistance to anti-neoplastic therapy (Brabletz *et al*.; 2018). Among the EMT responsible genes, there is a family of proteins involved in the formation of Tight Junctions (TJs) whose expression is altered in different tumors including thyroid carcinoma (Gonzalez-Mariscal *et al*.; 2007).

TJs are cellular junctions located in the most apical area of epithelial or endothelial cells and can be sub-divided into the integral membrane and cytoplasmic proteins. TJ perform different functions, in particular regulate the permeability of solutes between adjacent cells and direct the lateral diffusion of proteins within the lipid bilayer (Runkle *et al*.; 2013).

Junctional Adhesion Molecules A (JAM-A, also Known as F11R) belong to immunoglobulin superfamily of adhesion molecules (Chiba *et al*.; 2008). Three different proteins have been identified as belonging to this superfamily: JAM-A, JAM-B and JAM-C which share ~ 32-38% homology (Aurrand- Lions *et al*.; 2000; Martin-Padura *et al*.; 1998). In particular, JAM-A is located near the

junctions of endothelial and epithelial cells and is predominately expressed in endothelial cells, in epithelial tight junction, in neutrophils and lymphocytes. JAM-A was originally described as a receptor capable of binding to a monoclonal antibody that can induce platelet aggregation (Steinbacher *et al*.; 2017). JAM-A is an important regulator of the polarity of epithelial and endothelial cells and participates in different process including regulation of EMT activation of platelets, transmigration of monocytes and angiogenesis (Keiper *et al*.; 2005). JAM-A is composed of an extracellular domain capable of interacting with immunoglobulin antibodies (Ig), a single trans-membrane region and a small intracytoplasmic piece that ends with a PDZ (Platelet Derived Zimogen) domain able to interact with cytosolic proteins (Liu *et al*.; 2010). Through the Ig domain, JAM-A protein mediates the formation of cell-cell adhesions forming both homodimer and heterodimeric interactions (binding to platelets or membrane integrin). The cytoplasmic domain, although it doesn't have catalytic activity, plays a fundamental role for the biological activity of JAM-A because it contains different interaction sites for different proteins. These proteins include Afadina, ZO-1, ZO-2 (zonula occludens protein 1-2), CASK (calcium/calmodulin dependent serine protein kinase), PAR-3 (partitioning-defective 3 homolog), MUPP1 (multiple PDZ domain protein), PICK-1 (protein interacting with C kinase 1) and RAPGEF (Rap guanine nucleotide exchange factor 6) proteins. In particular the interaction of JAM-A with the Afadina protein seems to regulate cell migration, while the lack of interaction with the ZO-1 and ZO-2 proteins does not allow the assembly of tight junctions (Steinbacher *et al*.; 2017).

In Figure 3 are shown the structure and the signaling model of JAM-A.

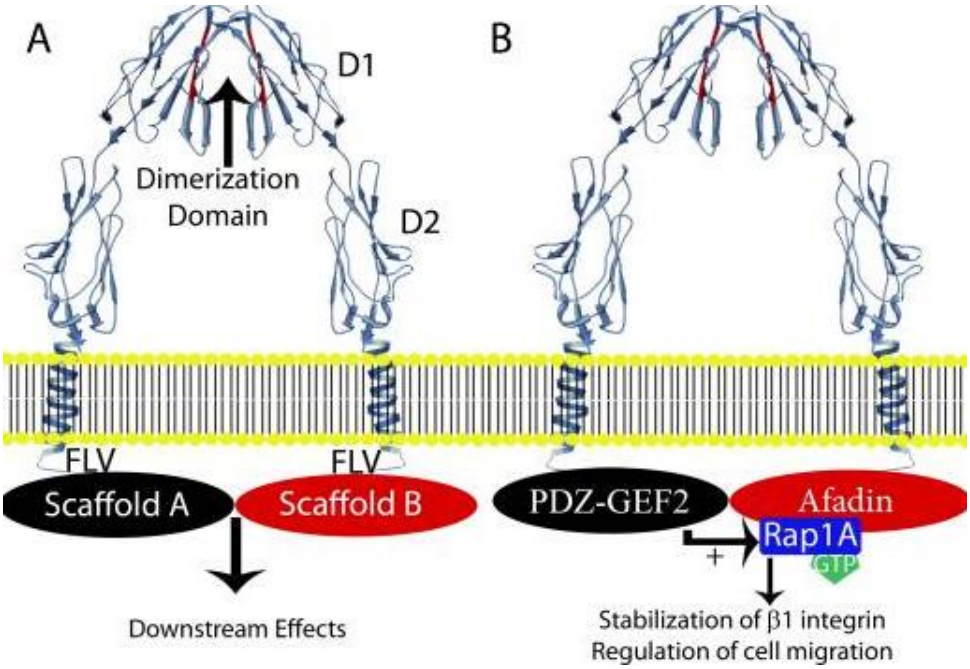

Figure 3. Structure of JAM-A and JAM-A signaling model. JAM-A (crystal structure in blue) has two extracellular Ig-like loops, the membrane distal domain D1 and the membrane proximal domain D2. Dimerization of JAM-A is mediated through binding interactions with D1 and brings into close apposition two PDZ-binding domains that facilitate the formation of PDZ containing scaffold protein complexes and subsequent signaling events. b) Model of outside-in signaling through JAM-A that regulates epithelial cell migration. In this model, dimerized JAM-A brings into close apposition Afadin/Rap1A and PDZGEF2 to activate Rap1A. The active GTPase acts to stabilize cell surface β1 integrin protein and regulate cell migration (Severson *et al*.; 2009).

JAM-A is deregulated in many aggressive and metastatic human tumors. Low expression of this protein is associated with a poor prognosis in pancreatic, renal, gastric and melanoma tumors (Fong *et al*.; 2012; Gutwain *et al*.; 2009; Kakuki *et al*.; 2016; Huang *et al*.; 2014), while overexpression of JAM-A correlates with tumor progression and poor prognosis in non-small cell lung cancer and testicular cancer (Zhang *et al*.; 2013; Tarulli *et al*.; 2013). Both overexpression and underexpression of JAM-A has been observed in breast cancer. In fact, in one study it was shown that this protein reduces the motility and invasiveness of tumor cell lines and its expression is inversely related to aggressiveness in breast cancer tissue samples (Naik *et al*.; 2008). While in other works the increase

of expression of JAM-A protein has been reported to be related to a poor prognosis in breast cancer patients (McSherry *et al*.; 2009).

RESULTS (I)

1. TUSC2 impairs proliferation and motility of thyroid cancer cells

To evaluate, *in vitro*, the biological function of the tumor suppressor TUSC2 in thyroid carcinogenesis, anaplastic thyroid cells 8505C, expressing low level of TUSC2, was stably transfected with the TUSC2 plasmid and the corresponding control vector (named Control Vector). A mass population, expressing high level of TUSC2 was chosen to conduct functional experiments. First, we asked whether, in these cell line, TUSC2 forced expression affects cell proliferation rate. For this purpose, we have conducted a methyl tetrazolium compound assay (MTS) assay and we have demonstrated that TUSC2 reduced proliferation in 8505C cells respect the control cells (Figure 1).

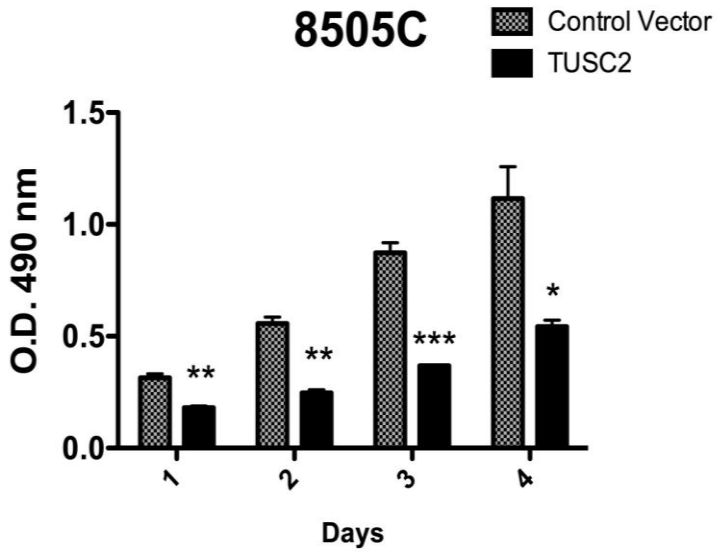

Figure 1: TUSC2 overexpression reduced thyroid cancer cell proliferation. Cell proliferation was measured by MTT assay. Absorbance was measured at O.D.490 nm every 24 hours for four days. The data are average of three independent experiments ± standard errors. *$p < 0.05$, **$p < 0.01$, ***$p < 0.001$ *(modified from Mariniello et al.;2020).*

Finally, we studied the effects of overexpression of TUSC2, in 8505C cell line stably transfected, on cell cycle progression by flow cytometry with propidium iodide (PI) staining. As shown in Figure 2a, we have demonstrated that TUSC2 caused an accumulation of the cells in the G2/M phase. Then we have also analyzed the expression level of proteins involved in the cell cycle regulation such as p21, p27 and CDK6. Through Western blot analysis we showed that p21 and CDK6 were decreased while p27 expression was increased in 8505C cells transfected with TUSC2 plasmid respect to control (Figure 2b).

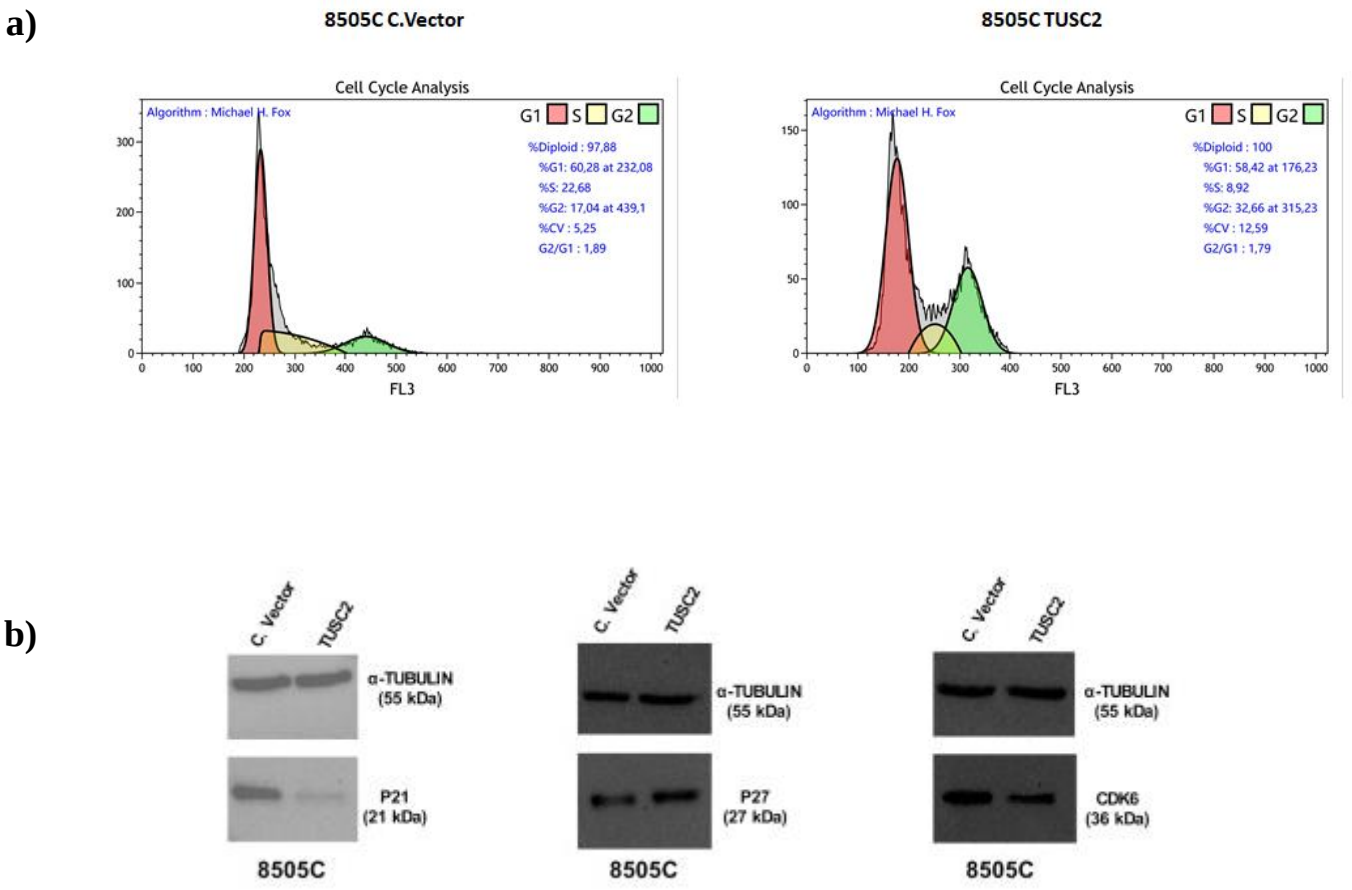

Figure 2: Overexpression of TUSC2 reduced cancer cell proliferation. a) Flow cytometry analysis in 8505C/TUSC2 cell line respect to cells transfected with control vector. **b)** Western blot of p21,p27 and CDK6. Tubulin was used as normalizer *(modified from Mariniello et al.;2020).*

To evaluate the role of TUSC2 on migration and invasion ability we performed a wound healing and Matrigel matrix assay respectively. For wound healing, a scraped wound was introduced on the confluent monolayer of 8505C/TUSC2 cells transfected with specific plasmid or control vector, and the cell migration was monitored for 24 hours. 8505C cell line transfected with the control vector efficiently migrated into the wound; by contrast, cells transfected with TUSC2 show a reduced migrating ability (Figure 3).

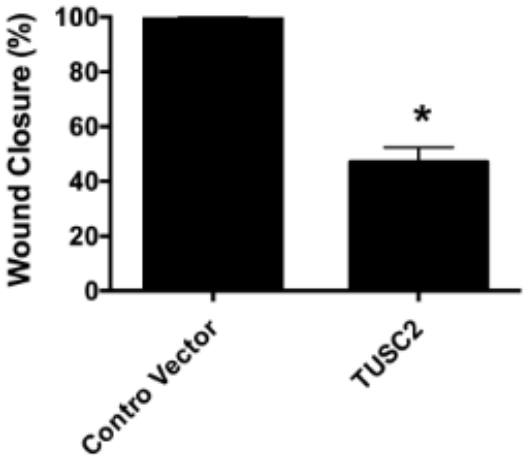

Figure 3: TUSC2 forced expression reduced thyroid cancer cell migration. A wound was introduced on a confluent monolayer of 8505C cells stably transfected with TUSC2 plasmid or Control Vector, and cell migration into the wound was monitored for 24 hours. Wound closure was measured by calculating pixel densities in the wound area and expressed as percentage ± standard errors *$p < 0.05$ *(modified from Mariniello et al.;2020)*

We, then, evaluated cell invasion in Matrigel matrix. To this aim the cells were plated on the surface of Transwell coated with Matrigel matrix and after 24 hours the invaded cells were stained, photographed and quantified. As shown in Figure 4, TUSC2 reduced ability to invade Matrigel in 8505C cells respect cells transfected with control vector.

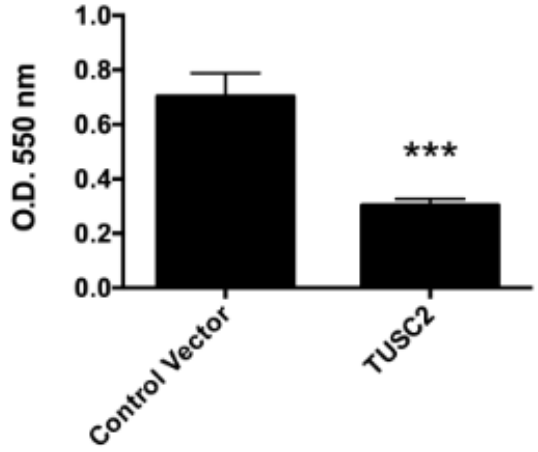

Figure 4: TUSC2 forced expression reduced thyroid cancer cell invasion. 8505C transfected cells were seeded in the upper chambers of Transwells coated with Matrigel and incubated for 24 hours; the upper surface of the filter was cleaned and cells on the lower surface were stained and quantified measuring absorbance at 550 nm *(modified from Mariniello et al.;2020).*

The obtained results indicate that TUSC2 restoration decreased the migration and invasion of thyroid cancer cell lines.

Furthermore, all these results were confirmed in TPC-1, another cell line that is derived from papillary thyroid carcinoma (data not shown).

2. Identification of proteins activated by TUSC2 in response to apoptotic stimuli in thyroid cancer cells

To investigate the molecular mechanisms through which TUSC2 acts, we analyze the effect of this tumor suppressor in the apoptosis process. For this purpose, we treated the 8505C/TUSC2 and 8505C/ Control Vector cells with staurosporine (2.5 µM), for 24 hours. We have analyzed, concurrently, 43 human apoptotic markers through Proteome Profiler Human Apoptosis Array (R&D Systems).

The results shows that in 8505C/TUSC2 cells treated with staurosporine (STS), the expression levels of the apoptotic proteins SMAC/DIABLO and CYTOCHROME C were increased respect control cells (Figure 5). This data has been confirmed by western blot (data not shown).

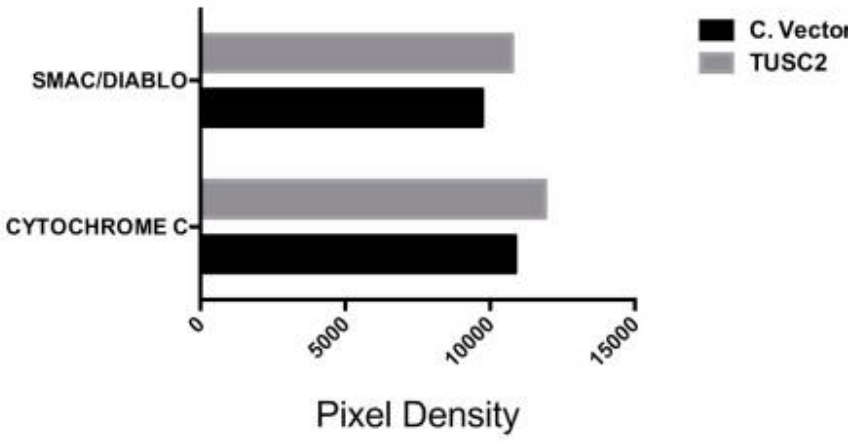

Figure 5: TUSC2 forced expression increased SMAC/DIABLO and CYTOCHROME C protein levels. 8505C /TUSC2 and 8505C/ Control Vector were treated with 2.5 µM STS. After 24 hours from treatment protein lysates were blotted on the Proteome Profiler Human Apoptosis Array nitrocellulose membrane. Quantification of pixel intensities was performed with the ImageJ software program (version 1.50i). Pixel density was normalized by subtracting the average background signal. *(modified from Mariniello et al.;2020).*

3. TUSC2 silencing increased the malignant phenotype of the Nthy-ori 3-1 cell line

Furthermore, we silenced TUSC2 in Nthy-ori 3-1 cell line by using two different TUSC2 siRNA (named 5 and 6) designed to specifically bind and inhibit endogenous level of this tumor suppressor. After 72 hours of transient transfection, cells were screened by western blot for TUSC2 expression. We performed, in these cell lines, the specular experiments to verify the previous results. We evaluated migration capacity through Wound healing assay. In particular, the experiment was performed 24 hours after transient transfection. As shown in Figure 6, silencing of TUSC2 increased migration ability of Nthy-ori 3-1 cells respect to cells transiently transfected with Control siRNA.

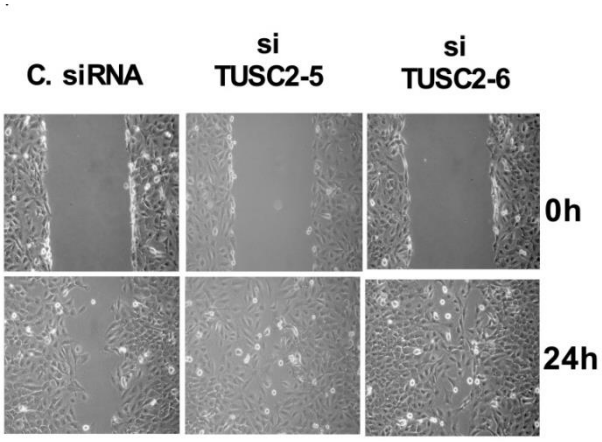

Figure 6: TUSC2 silencing increased migration ability of the Nthy-ori 3-1 cell line. Representative images of scratch wound healing assay of Nthy-ori 3-1 transfected with siRNA of TUSC2 and respective vector control *(modified from Mariniello et al.;2020).*

Invasion assay in Matrigel matrix assay demonstrated that low expression level of TUSC2 increases the ability of these cells to invade (data not shown).

Finally, I have evaluated the effect of silencing of TUSC2 on cell proliferation. To this purpose, Nthy-ori 3-1 cell line, transiently transfected with siRNA TUSC-5 and siRNA TUSC-6 and relative control, were treated with doxorubicin (for 48 hours) and staurosporine (for 24 hours) and a trypan blue assay was performed. As shown in Figure 7, silencing of TUSC2 increase the cell number respect to the corresponding control cells.

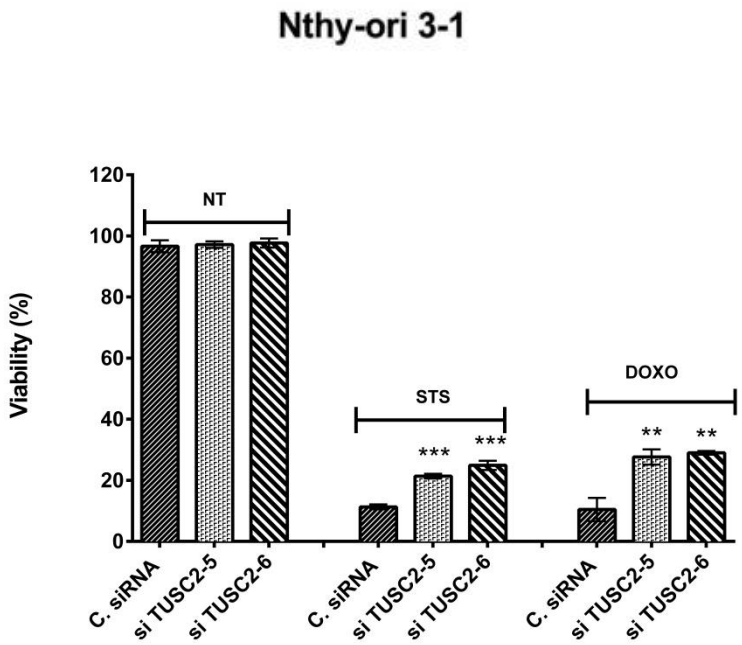

Figure 7: TUSC2 silencing increase resistance to apoptosis in thyroid cancer cells. The Nthy-ori 3-1 cell line was transiently transfected with specific siRNA. 24 hours after transfection, cells were treated with 1 µM of DOXO for 24 hours or with 2.5 µM of STS for 24 hours. Successively cells were stained with trypan blue and counted. The results represent the percentages of cells viability. Values are the average of duplicate experiments ± standard errors. ** $p < 0.01$ and *** $p < 0.001$ *(modified from Mariniello et al.;2020).*

All together, these results established the role of TUSC2 as a tumor suppressor protein in human thyroid carcinogenesis.

4. SMAC/DIABLO mediates in part TUSC2 effects

Finally, we asked if SMAC/DIABLO could mediate the biological phenotype induced by TUSC2. To this aim, we silenced SMAC/DIABLO in 8505C/TUSC2 and in 8505C/C.Vector cells. Silencing of SMAC/DIABLO was performed using two different siRNAS -5 and -6. Through cell viability assay (Figure 8a) and wound healing assay we have demonstrated that silencing of SMAC/DIABLO partially rescued the effect induced by TUSC2 (Figure 8b)

.

8505C

a)

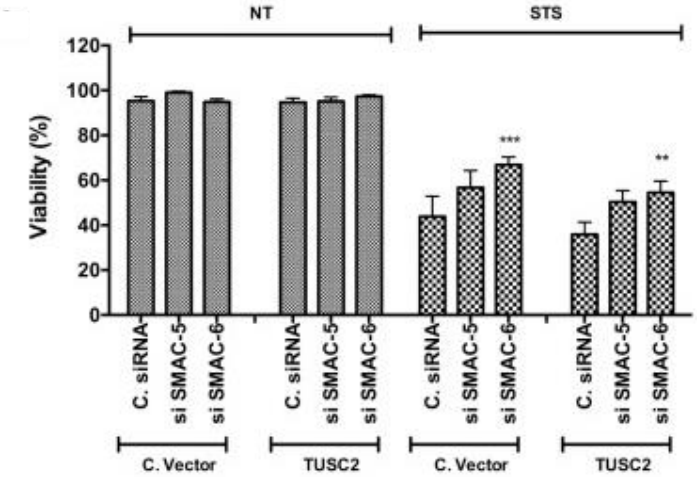

b)

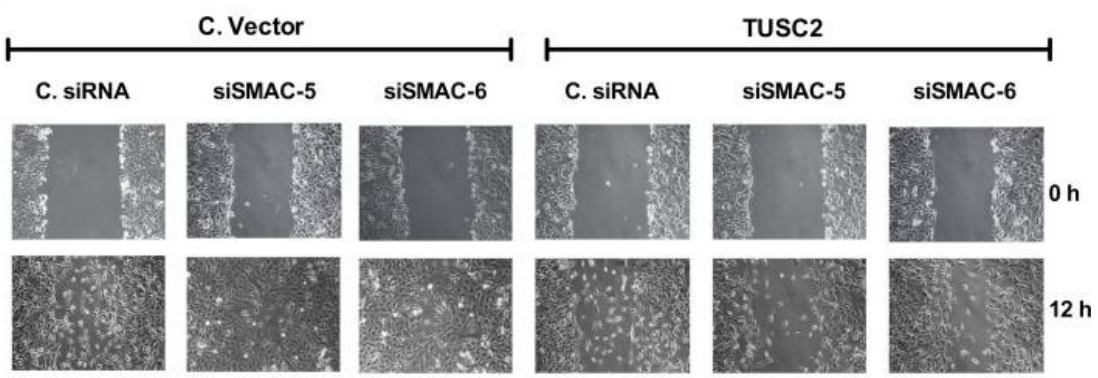

Figure 8: Silencing SMAC/DIABLO partially rescues the TUSC2-induced phenotype in the 8505C cell line. a) 8505C/C. vector and 8505C/TUSC2 cell lines were transiently transfected with the specific siRNA of SMAC/DIABLO. The day after transfection, the cells were treated with STS for 24 hours. After treatment cells were stained with trypan blue and counted. **b)** 8505C/C. vector and 8505C/TUSC2 cell lines were transiently transfected with the SMAC/DIABLO siRNA and, 24 hours post transfection, a scratch wound was generated on the confluent monolayer. The wound closure was monitored for 24 hours and distance of scratch was quantified by calculating pixel densities in the wound area and expressed as the percentage of wound closure. Values represent the average of duplicate experiments ± standard errors. ** $p < 0.01$ and *** $p < 0.001$*(Modified from Mariniello et al.;2020).*

Finally we have confirmed all these results in Nthy-ori 3-1 cell lines. Initially we have silenced TUSC2 (using TUSC2 siRNAs) and we evaluated the expression levels of SMAC/DIABLO and CYTOCHROME C. According to the results shown below, the level of these apoptotic proteins decreased in Nthy-ori 3-1 siTUSC2 respect to cells transfected with control siRNA (Figure 9).

Nthy-ori 3-1

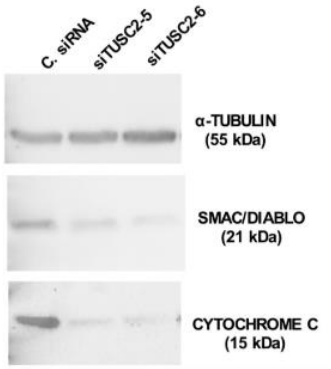

Figure 9: TUSC2 silencing decreased expression level of SMAC/DIABLO and CYTOCHROME C in Nthy-ori 3-1 cell line. Immunoblotting of SMAC/DIABLO and CYTOCHROME C and α-Tubulin in Nthy-ori 3-1 transiently transfected with TUSC2 siRNAs *(modified from Mariniello et al.;2020).*

Accordingly, Nthy-ori 3-1 cells transiently silenced for TUSC2 has been also transfected with a SMAC/DIABLO encoding plasmid to evaluate migration ability through wound healing. As shown in Figure 10, forced expression of SMAC/DIABLO reversed the motility effects induced by silencing of TUSC2 in Nthy-ori 3-1 cells. These results suggest that SMAC/DIABLO is a mediator of TUSC2 biological effects in thyroid cancer cells.

Nthy-ori 3-1

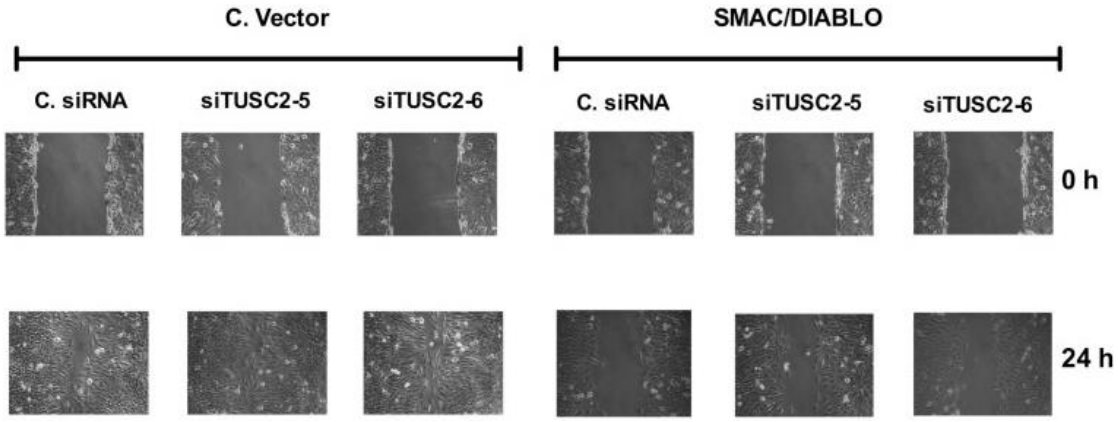

Figure 10: SMAC/DIABLO partially rescued the TUSC2 induced phenotype in the cell line. A wound was made in a confluent monolayer of Nthy-ori 3-1 (co-transfected with siRNAs TUSC2 and SMAC/DIABLO plasmid) cells by scratching using a pipette tip. After 24 hours, migrating cells was photographed *(modified from Mariniello et al.;2020).*

Overall, the results obtained clarified a role of TUSC2 in thyroid cancer cells as possible novel biomarker for thyroid carcinomas and as possible therapeutic target. Additionally, these results demonstrated that SMAC/DIABLO is a mediator of TUSC2 induced effects in thyroid cancer cells.

RESULTS (II)

1. Identification of EMT-related genes in thyroid carcinoma

To further dissect the molecular mechanisms involved in thyroid neoplastic transformation, during my PhD, I focused my work on the study of the epithelial-mesenchymal transition (EMT) a key process involved in neoplastic progression and metastatic dissemination (Montemayor-Garcia *et al*.; 2013).

The research group, where I performed my PhD work, decided to analyze the expression profile of the genes involved in EMT, in order to identify new markers of thyroid cancer progression.

For this purpose, we used the EMT-Profiler PCR Array (Qiagen) to characterize the gene expression profile of EMT-related genes in 9 anaplastic thyroid cancer (ATC), 11 papillary thyroid cancer (PTC), and 9 normal thyroid tissues (NT). Through PCR array we analyze the expression of 84 genes whose role in EMT is already known in the literature; in addition, the 84 genes are divided, by the manufacture, into different groups based on their biological function (Table 2).

Table 2: Functional groups of EMT-RT2 ProfilerTM PCR Array (provided of Qiagen) (*Orlandella et al.;2019).*

	Gene List
Extracellular Matrix & Cell Adhesion Molecules	BMP1, BMP7, CDH1 (E-Cadherin), CDH2 (N-Cadherin), COL1A2, COL3A1, COL5A2, CTNNB1, DSC2, EGFR (ERBB1), ERBB3, **F11R**, FN1, FOXC2, ILK, ITGA5, ITGAV, ITGB1, MMP2, MMP3, MMP9, PTK2 (FAK), RAC1, SERPINE1 (PAI-1), SPP1, TGFB1, TGFB2, TIMP1, VCAN.
Up-Regulated During EMT	AHNAK, BMP1, CALD1, CAMK2N1, CDH2 (N-Cadherin), COL1A2, COL3A1, COL5A2, FN1, FOXC2, GNG11, GSC, IGFBP4, ITGA5, ITGAV, MMP2, MMP3, MMP9, MSN, SERPINE1 (PAI-1), SNAI1 (SNAIL), SNAI2, SNAI3, SOX10, SPARC, STEAP1, TCF4, TIMP1, TMEFF1, TMEM132A, TWIST1, VCAN, VIM, VPS13A, WNT5A, WNT5B
Down-Regulated During EMT	CAV2, CDH1 (E-Cadherin), DSP, FGFBP1, IL1RN, KRT19, MST1R (RON), NUDT13, OCLN, DESI1, RGS2, SPP1, TFPI2, TSPAN13.
Differentiation & Development	AKT1, BMP1, BMP2, BMP7, COL3A1, COL5A2, CTNNB1, DSP, ERBB3, **F11R**, FOXC2, FZD7, GSC, JAG1, KRT14, MST1R (RON), NODAL, NOTCH1, PTP4A1, SMAD2 (MADH2), SNAI1 (SNAIL), SNAI2, SOX10, TGFB2, TGFB3, TMEFF1, TWIST1, VCAN, WNT11, WNT5A, WNT5B.
Cell Morphogenesis	CTNNB1, FOXC2, JAG1, RAC1, SMAD2 (MADH2), SNAI1 (SNAIL), SOX10, TGFB1, TGFB2, TGFB3, TWIST1, WNT11, WNT5A.
Cell Growth & Proliferation	AKT1, BMP1, BMP7, CAV2, CTNNB1, EGFR (ERBB1), ERBB3, FGFBP1, FOXC2, IGFBP4, ILK, JAG1, MST1R (RON), NODAL, PDGFRB, TGFB1, TGFB2, TGFB3, TIMP1, VCAN, ZEB1.
Cell Migration & Motility	CALD1, CAV2, EGFR (ERBB1), FN1, ITGB1, JAG1, MSN, MST1R (RON), NODAL, PDGFRB, RAC1, STAT3, TGFB1, VIM.
Cytoskeleton Regulators	CAV2, KRT7, MAP1B, PLEK2, RAC1, VIM.
Transcription Factors	CTNNB1, ESR1 (ERα), FOXC2, GSC, NOTCH1, GEMIN2, SMAD2 (MADH2), SNAI2, SNAI3, SOX10, STAT3, TCF3, TCF4, TWIST1, ZEB1, ZEB2.

In particular, we analyzed the results obtained from the array q-RT-PCR and calculated the average expression of each gene, focusing in genes involved in cell adhesion and extracellular matrix formation in ATC and PTC compared to NT (Table 3). Among the genes differentially expressed we investigated JAM-A (alias F11R) because it was one of the most down-regulated genes in ATC respect to PTC and NT and because its role in thyroid cancer was to our knowledge unknown.

Table 3. Expression levels of "Extracellular Matrix & Cell Adhesion" molecules in thyroid carcinoma (*Orlandella et al.;2019).*

Gene Name	**Average Fold Change PTC (n= 11)**	**Average Fold Change ATC (n = 9)**
CDH1	1.3	0.4
BMP7	0.7	0.4
F11R	1.7	0.6
CTNNB1	1.9	0.6
RAC1	1.4	0.9
PTK2	1.4	1
ERBB3	3.3	1
EGFR	2.0	1.2
ITGAV	1.6	1.5
ILK	1.4	1.6
TGFB2	2.0	1.7
DSC2	3.7	1.7
ITGB1	1.9	2.0
MMP2	0.8	2.4
BMP1	3.3	2.5
ITGA5	1.9	2.8
FOXC2	0.9	3.6
TIMP1	7.0	4.3
TGFB1	3.0	6.1
MMP3	8.7	6.1
COL1A2	3.2	7.5
MMP9	1.9	7.7
COL5A2	2.5	7.8
CDH2	10.9	9.8
SPP1	2.4	10.1
VCAN	7.5	11.9
SERPINE	2.3	12.8
COL3A1	4.1	14.2
FN1	34.7	19.1

2. JAM-A is down-regulated in ATC samples

Based on the results obtained from previous analysis and because of the absence of study on the role of JAM-A in thyroid cancer, we investigated the biological function of this protein in thyroid neoplastic progression.

To confirm the down-regulation of JAM-A expression level obtained by EMT-array, we measured by qRT-PCR the level of JAM-A in ATC (n=5) with respect to PTC (n=12) and NT (n=7) thyroid tissues samples. As shown in Figure 11, JAM-A expression level was significantly lower of ~2 fold in ATC samples respect to PTC and NT.

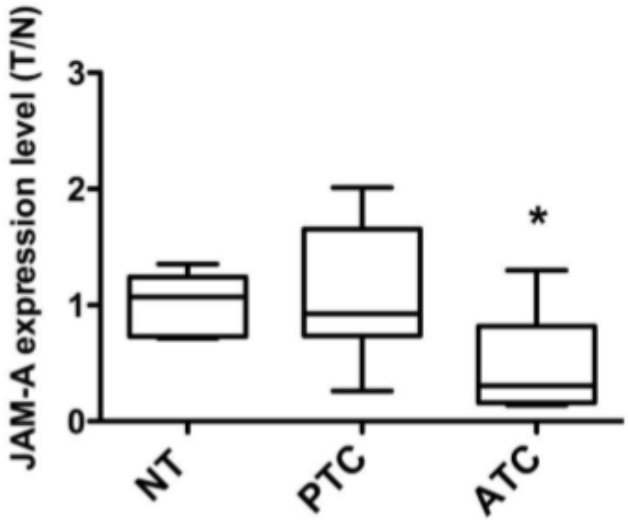

Figure 11: JAM-A is down-regulated in ATC samples. qRT-PCR of JAM-A in normal thyroids, PTC and ATC snap frozen tissue. The expression levels of JAM-A in each sample were measured comparing its fluorescence threshold with the average fluorescence threshold of the NT samples. The figure shows the average results of four independent experiments. *p <0.05 *(modified from Orlandella.;2019).*

We have also evaluated, by immunohistochemistry the expression level of JAM-A protein in a panel of human thyroid carcinoma tissues, including a positive control adenocarcinoma sample, normal thyroids (NT), PTCs and ATCs. As reported in Figure 12, all normal thyroids examined showed JAM-A positivity (89.4%). On the contrary JAM-A level was low in ATC tissues (14.6%) or undetectable in 81.2% of cases. An intermediate positivity of staining was seen in PTC. In particular for PTC classical variant samples, we observed high JAM-A expression in 64.3% and low or totally absent JAM-A expression in 35.7% (Table 5).

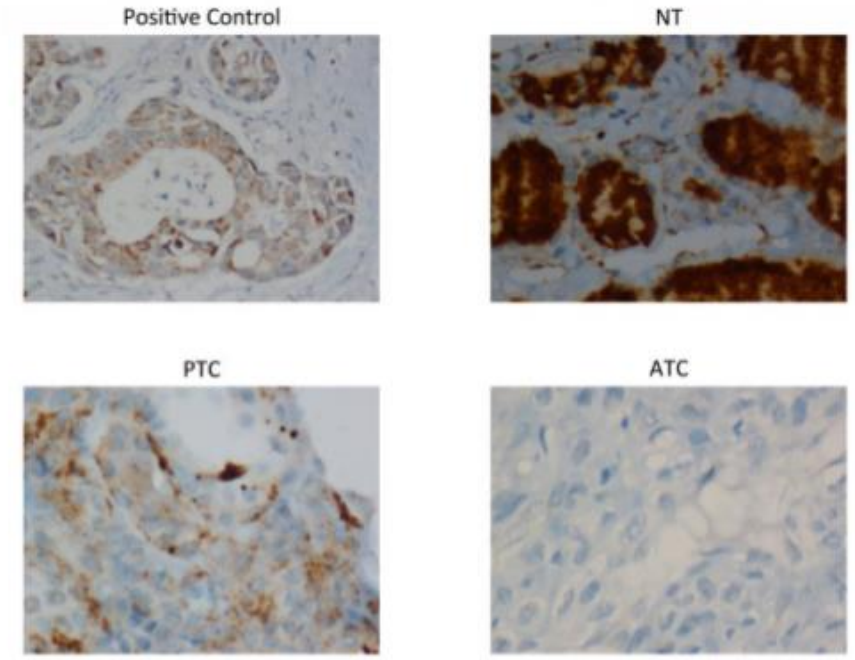

Figure 12. Expression of JAM-A in thyroid tissue samples. Immunohistochemical analysis of JAM-A protein expression in normal and malignant thyroid tissues. Representative histological sections from a positive control adenocarcinoma sample (10 X magnification), NT (40 X magnification), classical PTC (40 X magnification), and ATC stained with an anti-JAM-A antibody are shown *(modified from Orlandella et al.; 2019).*

Table 4: Expression of JAM-A in human thyroid samples by HIC (*Orlandella et al.; 2019).*

JAM-A	**NT (N = 19)**	**PTC (N=14)**	**ATC (N=48)**
+++	17 (89,4%)	4 (28,6%)	2 (4,2%)
++	1 (53%)	5 (35,7%)	-
+	1 (5,3%)	3 (21,4%)	7 (14,6%)
Negative	-	2 (14,3%)	39 (81,2%)

+, ≥ 5 a ≤ 25% of positive cells;
++, > 25 a < 60% of positive cells;
+++, ≥ 60 % of positive cells.

3. JAM-A forced expression impairs different hallmarks of thyroid cancer cell lines transformation

To investigate the biological role of JAM-A in thyroid carcinogenesis we stably transfected anaplastic thyroid cell lines CAL62, negative for expression of JAM-A, with plasmid encoding for JAM-A and corresponding control vector named Empty Control. After selection with puromycin, the transfection efficiency was analyzed through western blot. The mass population expressing high level of JAM-A was chosen for further experiments (Figure 13).

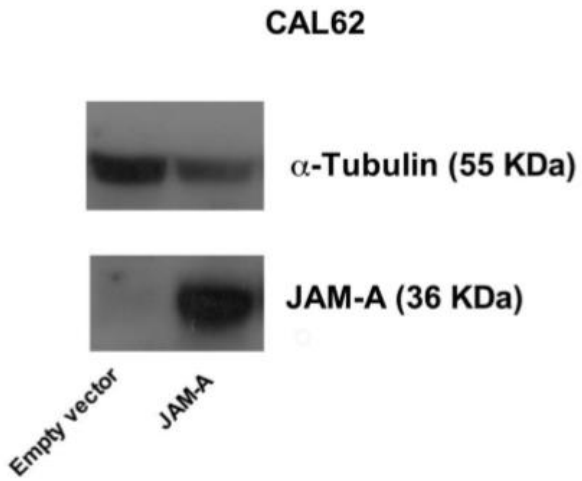

Figure 13: **CAL62 cells transfected with JAM-A express high levels of the protein respect cells transfected with the control vector.** The cells were lysed after stable transfection and analyzed by Western blot to evaluate the expression of the JAM-A protein. The expression of α-Tubulin was used as a normalizer *(modified from Orlandella et al.; 2019).*

We then studied the effects of JAM-A protein on cell proliferation. To this aim CAL62/JAM-A and respective control were plated at time 0 and counted at different time points (24, 48, 72 and 96 hours). As shown in Figure 14, in the cells that overexpress JAM-A the proliferation rate was significantly reduced respect to control.

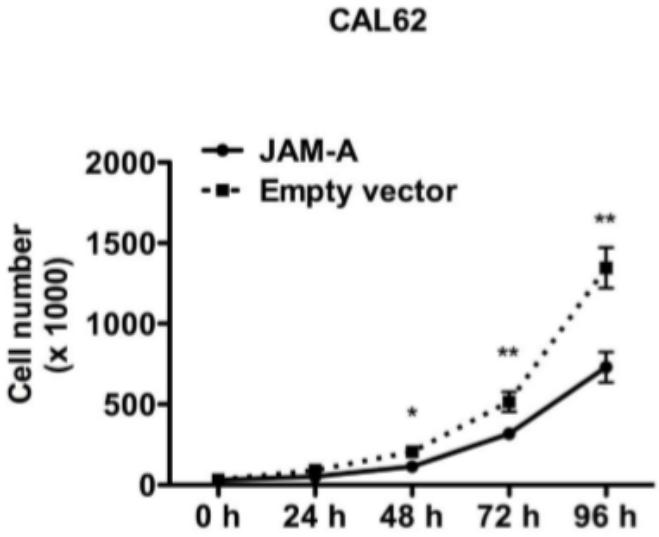

Figure 14: Forced expression of JAM-A decreased proliferation rate in ATC cells. CAL62 cells transfected with JAM-A or with the control plasmid were plated and counted at different time points. Values represent the average of triplicate experiments ± standard deviations. Asterisks indicate *p<0.05, **p <0.01 *(modified from Orlandella et al.; 2019).*

To confirm this result, we performed a colony formation assay. In this experiment CAL62 cells after transfection with JAM-A or with the control plasmid were selected with puromycin. Subsequently, the colonies were stained with crystal violet (Figure 15a) and counted (Figure 15b).

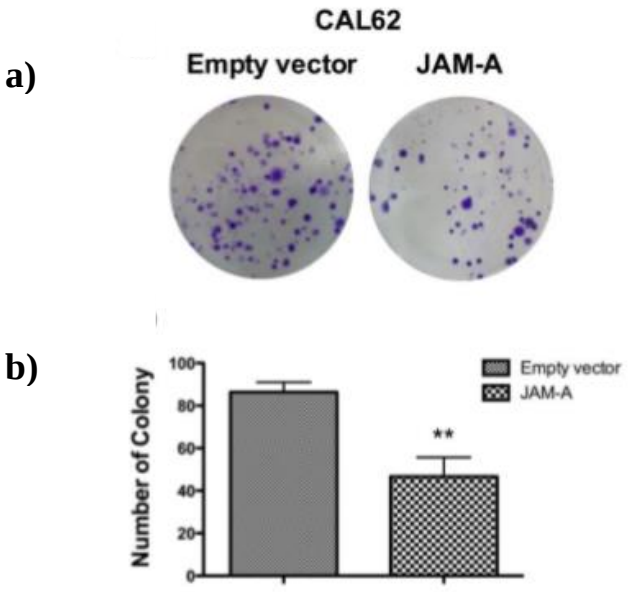

Figure15: Forced expression of JAM-A decreased proliferation rate in ATC cells. a) Representative image of the formation of colonies in CAL62 transfected with JAM-A or with control. b) Quantification of number of colony. The values represent the mean ± SD of three independent experiments. **p <0.01 *(modified from Orlandella et al.; 2019).*

The results obtain shows that cell lines transfected with JAM-A have a reduced number of colonies compared to the cells transfected with the empty vector.

All together these results demonstrates that JAM-A decreases the proliferative capacity of ATC cells. Subsequently, we evaluated the migration ability of JAM-A in CAL62 cells by wound-healing assay. For wound healing a scraped wound was introduced on the confluent monolayer of cells transfected with JAM-A and cells transfected with Empty vector. Cells were photographed at time zero and the scrape was monitored to closure at 24 hours. As shown in Figure 16, CAL62 transfected with JAM-A have a reduced migration ability respect cells transfected with Empty control vector. To exclude that difference in migration could be due to different cell growth, cells were treated with Mytomicin C that is a cytostatic antibiotic capable of blocking the cell cycle in the G1/S phase of the cell cycle.

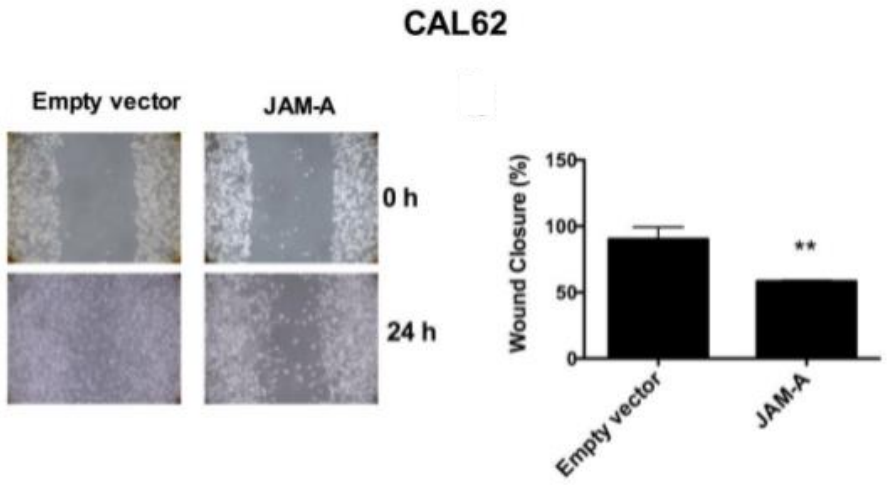

Figure 16: Forced expression of JAM-A reduced migration in ATC cells. Wound healing of CAL62 cells transfected with JAM-A. Cells were photographed at time zero and after 24 hours. Wound closure distance was quantified by calculating pixel densities in the wound area and expressed as a percentage of wound closure of the area. The values represent the average of experiments performed in triplicate ± SD. ** p <0.01 (*modified from Orlandella et al.; 2019).*

Furthermore, the invasive ability of CAL62 was analyzed by chemoinvasion assay using a membrane with characteristics similar to the extracellular matrix. In particular, CAL62/JAM-A and CAL62/Empty vector cells were plated in the upper chambers of Transwell coated with Matrigel and incubated 48 hours at 37°C. The cells that migrated on the lower surface were stained with Crystal Violet and quantized as absorbance at O.D 550 nm. As shown in Figure 17, cells transfected with JAM-A have a reduced ability to invade a Matrigel matrix compared to control cells.

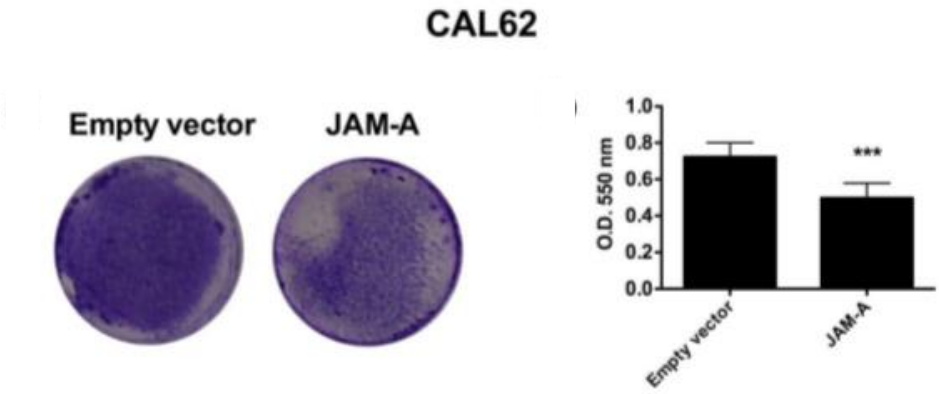

Figure 17: Overexpression of JAM-A reduced invasion in ATC cells. CAL62/JAM-A transfected cells were seeded in the upper chamber of Transwells coated with matrigel and incubated for 24 hours. The invasive ability is expressed as absorbance at OD 550 nm. Value represent the average of triplicate experiments ± SD ***p<0.001 *(modified from Orlandella et al.; 2019).*

Furthermore, similar experiments were conducted and the results were confirmed in OCUT-1, another anaplastic thyroid cancer cell line (data not shown).

4. JAM-A silencing increased proliferation and motility of TPC-1 cells

To confirm our findings, we performed the mirror experiment. To this aim we stably silenced JAM-A using specific shRNA in TPC-1 cells.

The stable silencing of JAM-A in TPC-1 induced an increased cell proliferation capacity measured by colony formation assay. As shown in Figure 28, TPC-1 cells transfected with sh JAM-A formed more colonies respect to cells transfected with the control (sh scrambled).

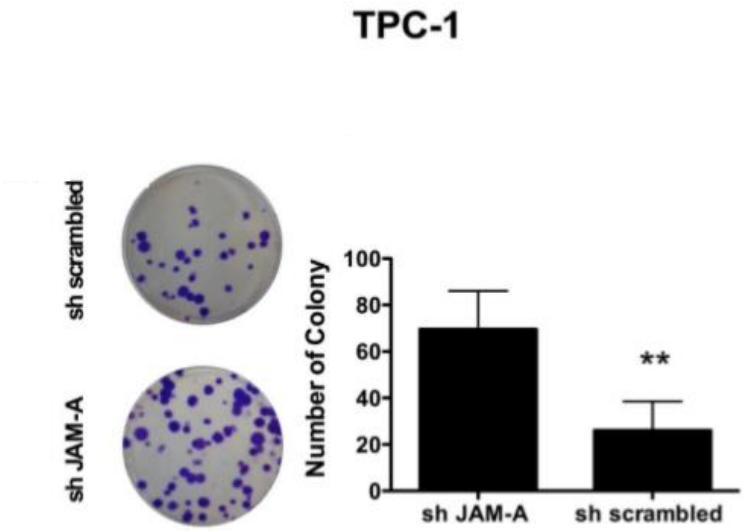

Figure 18: JAM-A silencing increased proliferation of TPC-1 cells. Representative image of colony formation in TPC-1 / sh JAM-A and TPC / sh scrambled cells (left) and quantitative analysis of the number of colonies (right). The values represent the average of three independent experiments ± SD. ** p <0.01 *(modified from Orlandella et al.; 2019).*

Moreover, silencing of JAM-A increased the ability of TPC-1 to migrate into wound. TPC-1/sh JAM-A cells migrate efficiently into the wound area after 24 hours, respect to TPC-1/sh scrambled cells, which exhibit extremely reduced migration ability (Figure 19).

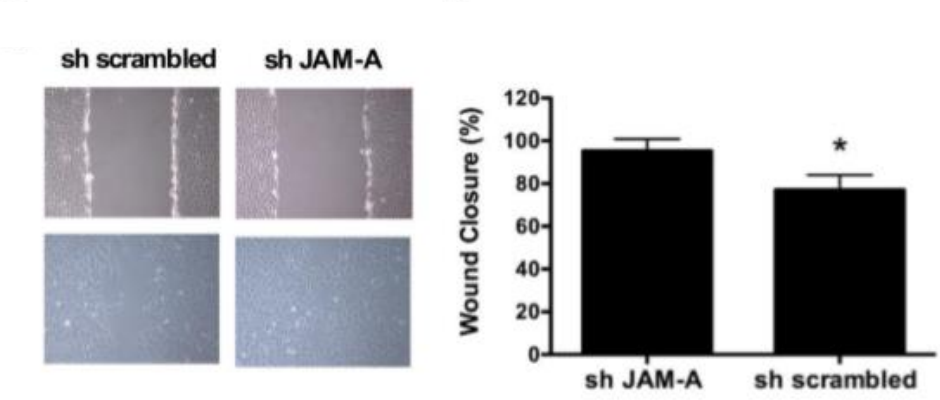

Figure 19: The cells transfected with sh JAM-A increased migration ability respect cell transfected with sh scrambled vector. Cells were plated and scratch wound were inflicted at confluent monolayer. After 24 hours, cells were photographed (left). The quantification is expressed as percentage of wound closure area (right). The values represent the average of experiments performed in triplicate ± SD *p <0.01 *(modified from Orlandella et al:;2019).*

Similarly the invasion ability was affected by JAM-A silencing (data not shown).

5. JAM-A impairs trans-endothelial migration and anchorage-independent growth of CAL62 cells

Finally, we studied the cell ability to penetrate into the endothelium by a trans-endothelial cell migration assay. CAL62/JAM-A cells and relative control were plated on confluent monolayer of HUVECs. As shown in Figure 20a, CAL62/JAM-A cells presented a reduced ability to migrate through endothelial cells compared with control cells. In addition, we explored if JAM-A affected anchorage-independent cell growth by soft agar. As shown in Figure 20b, CAL62/JAM-A produced less and smaller colonies in the semisolid medium when compared with control cells.

a)

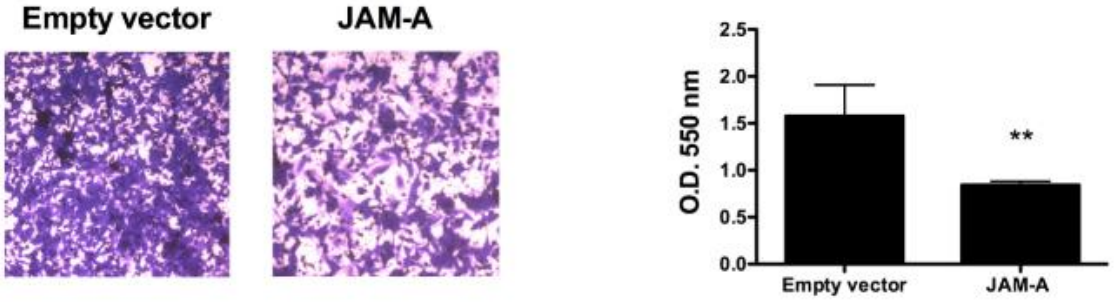

b)

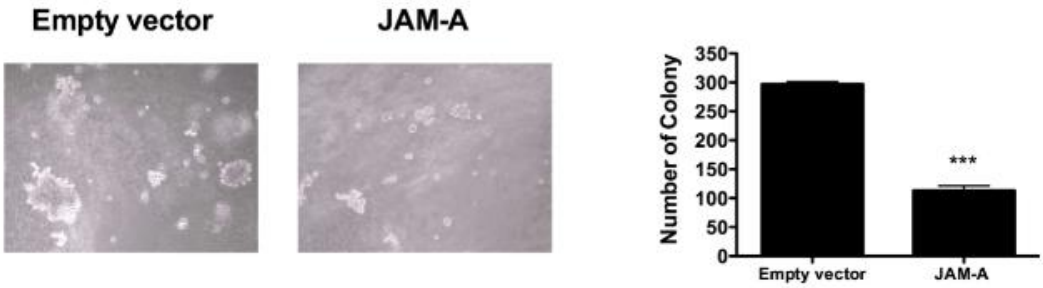

Figure 20: Overexpression of JAM-A suppressed trans-endothelial migration and colony formation in ATC cells. a) CAL62 transfected cells were seeded on a confluent monolayer of endothelial human umbilical vein endothelial cells (HUVECs) and left to migrate. Migration ability through HUVECs is expressed as absorbance at OD 550 nm. **b)** Anchorage-independent cell growth capability in soft agar. In figure is shown the image of colony formation of CAL62 stably transfected with JAM-A and with Empty Vector (left) and relative quantification (right). ** p <0.01 and ***p<0.001 *(from Orlandella et al:;2019).*

6. The expression of JAM-A regulates the signaling pathway of p53 and GSK3 α / β

To identify the signaling pathways regulated by the JAM-A protein in thyroid cancer, I screened, simultaneously, the phosphorylation status of 43 proteins using the Human Phospho-Kinase Array (R&D Systems, Minneapolis, MN, USA) in CAL62/JAM-A and CAL62/Empty vector cells. The

array is composed of two membranes on which primary antibodies specific for 43 different phosphoproteins are spotted. The membranes were incubated with the cell lysates obtained from the CAL62 transfected with JAM-A or with the empty vector. As shown in Figure 21, we found increased phosphorylation levels of p53 (at Serine 392) and of GSK3 α/β (at Serine 21 and Serine 9) in CAL62 cells overexpressing JAM-A.

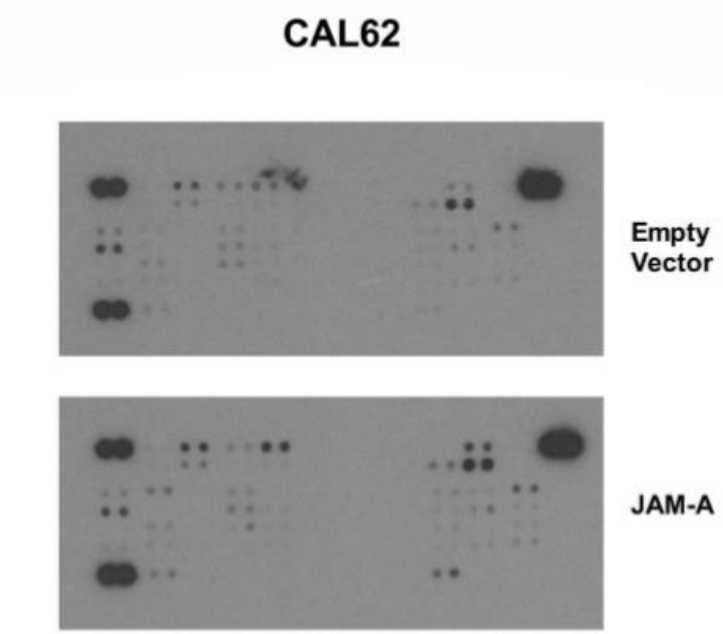

Figure 21. The JAM-A protein increases the phosphorylation of p53 on Serine 392 and GSK3 α / β on Serine 21/9 in CAL62 cells. The Human Phospho-Kinase Array was hybridized on CAL62 /JAM-A cells and CAL62/ Empty Vector cells. The membranes were incubated with 500 μg of cell lysate. Each antibody, which binds to specific phosphoproteins, is spotted in duplicate and detected by luminescent reagents *(modified from Orlandella et al:;2019).*

We also confirmed these results by Western blot analysis on an independent cell lysate of CAL62/JAM-A cells and CAL62/Empty Vector cells (data not shown).

Thus, overall these results showed that the adhesion molecule JAM-A affects multiple hallmarks of thyroid neoplastic transformation.

Discussion

Thyroid cancer is among the most frequent endocrine neoplasms, with an increase incidence in recent years. Thyroid carcinomas, that originate from follicular cells represent ~ 95% of all thyroid tumors and according to the clinical-pathological characteristics are classified in: well-differentiated carcinomas that include papillary thyroid carcinoma (PTC), hurthle cells carcinomas (HCC) and follicular thyroid carcinoma (FTC); poorly differentiated thyroid carcinomas (PDTC) and undifferentiated or anaplastic thyroid carcinomas (ATC) (Celano *et al*.; 2017). While well-differentiated carcinomas are generally curable with surgery and radioiodine therapy, anaplastic thyroid carcinomas are the most aggressive type of thyroid cancer, refractory to radioiodine treatment thereby limiting the efficacy of therapeutic interventions (Fuziwara *et al*.; 2014). For this reason, novel treatment approaches are needed for anaplastic thyroid cancer. To this aim it will be important to clarity the mechanisms underlying thyroid progression from well-differentiated to undifferentiated cancer.

During my PhD course, I have evaluated the role of TUSC2 in thyroid cancer because in previous studies conducted in the research laboratory where I performed my work, it was demonstrated that over-expression of miR-584 inhibits synthesis of the TUSC2 protein by targeting the 3'UTR of TUSC2 in thyroid cancer cell lines (Orlandella *et al*.;2016).

TUSC2, also known as FUS1, is located on human chromosome 3p21.3 and acts as a tumor suppressor in several human tumors (Lerman *et al*.; 2000). Genes in the 3p21.3 region are associated with cell differentiation, cell proliferation, apoptosis, and cell death (Ji *et al*.; 2005). Overexpression of TUSC2 significantly inhibits tumor growth and progression in mouse models and TUSC2 knockout mice show an increased frequency of spontaneous cancers (Ivanova *et al*.; 2007). The 3'UTR of TUSC2 is highly conserved, strongly suggesting that it plays an important role in regulating TUSC2 expression. Loss or reduction in TUSC2 expression has been observed in non-small cell lung carcinomas (NSCLC) (Prudkin *et al*.; 2008), mesothelioma (Iavanova *et al*.; 2009), esophageal

carcinoma (Zhang *et al*.; 2013), in glioblastoma (Xin *et al*.; 2015) and in sarcomas (Li *et al*.;2011). These observations support the role of TUSC2 as a tumor suppressor in human carcinogenesis. Previous studies in my research group demonstrated that TUSC2 was down-regulated in almost all ATC sample and in the majority of PTC samples (Orlandella *et al*.; 2016). During my PhD studies we shed light on the role of TUSC2 on thyroid cancer cell migration, invasion and resistance to apoptosis.

This dissertation is focused on unraveling the molecular mechanisms responsible for TUSC2 biological effects in thyroid cancer cells. To achieve this goal, we have analyzed the forced expression of TUSC2 in papillary (TPC-1) and anaplastic (8505C) thyroid cancer cell lines demonstrating *in vitro* that TUSC2 overexpression decreased growth by arresting the cell cycle progression and by reducing migration and invasion. These results are in agreement with Kondo and colleagues that demonstrated that TUSC2 over-expression decreased colony formation and was associated with an alteration of cell cycle kinetics in lung cancer cells (Li *et al*.;2014). Moreover, it has been demonstrated that TUSC2 has pro-apoptotic activity in human lung cancer cells. TUSC2 actives STAT-1 signal pathway and regulates the protein kinases EGFR, PDGFR, AKT, c-ABL and c-KIT (Dai *et al*.; 2015). During my PhD work we found that in 8505C/TUSC2 cells, in response to apoptotic stimuli, TUSC2 increased sensitivity to apoptosis by increasing the SMAC/DIABLO and CYTOCHROME C proteins. According to our results, the paper of Yazlovitskaya *et al*.; reported that in a TUSC2 knockout mouse model, cells presented low level of CYTOCHROME C (Yazlovitskaya *et al*.;2014). Considering that in literature the role of CYTOCHROME C is already known, during my studies I explored the role of SMAC/DIABLO on the TUSC2 biological effects demonstrating that the modulation of SMAC/DIABLO rescued the phenotype induced by TUSC2 protein in thyroid cancer cell lines. Indeed, we showed that TUSC2 is able to increase the expression levels of SMAC/DIABLO that sensitize cancer cells apoptosis following treatment with staurosporine.

Thus we clarify the mechanisms down-stream TUSC2. On the other hand, the mechanisms responsible of TUSC2 regulation are partially known. Loss or reduced TUSC2 expression could be

caused by various mechanisms. Uno et al., showed that one mechanism regulating TUSC2 expression and function is associated to loss of myristoylation of TUSC2 protein that removes its ability to suppress tumor growth (Uno *et al*.; 2004). In literature has been demonstrated that allelic loss of the 3p21.3 chromosomal region containing TUSC2 is the major cause of loss or reduction of TUSC2 expression in lung cancer (Prudkin *et al*.; 2008). In other type of tumor, the loss or reduction in TUSC2 expression can be regulate by several microRNAs. In particular the oncogenic activities of miR-92, miR-97 and miR-197 in lung cancer are mediated by silencing of TUSC2 (Du *et al*.;2009). In ovarian and nasopharyngeal cancers, it has been reported that miR-663 inhibits TUSC2 promoting cell growth, migration and invasion (Liang *et al*.;2017; Xie *et al*.;2019). Finally, Lee and colleagues proved that miR-378 promotes cell survival, tumor growth and angiogenesis by targeting TUSC2 (Lee *et al*.; 2007). Similarly, in thyroid cancer my research group reported that overexpression of miR-584 inhibits synthesis of the TUSC2 protein by targeting the 3'UTR of TUSC2. Importantly, TUSC2 is progressively downregulated in PTC and ATC tissues suggesting that TUSC2 is also likely to be involved in thyroid cancer progression, with implications for TUSC2 targeting as a rational therapeutic strategy in ATC (Orlandella *et al*.; 2016).

In addition, I focused my work on identifying others molecular determinants of thyroid cancer progression. In particular, one of the most important characteristics of thyroid cancer progression is that the anaplastic cells lose all the normal biological and functional characteristics of the normal thyroid follicular cells, as the ability to incorporate iodine, the ability to synthesize thyroglobulin and the dependence from TSH (Thyroid Stimulating Hormone) (Molinaro *et al*., 2017) and acquire a mesenchymal phenotype.

Epithelial mesenchymal transition (EMT) represents a fundamental process for tumor progression in ATC; it consists in the transformation of an epithelial cell into a cell with mesenchymal phenotype. To elucidate the molecular mechanisms underlying the EMT process in thyroid tumor progression, we performed an EMT Profiler PCR Array.

Among the genes differently expressed in PCR EMT Array we have identified two under-expressed genes in the ATC: CDH1 and BMP7. CDH1 encodes for E-Cadherin, and its low expression is considered a marker for EMT. In addition, the effect of the absence of E-Cadherin in ATC has already been reported in the literature (Liu *et al*.; 2010; Aratake *et al*.; 2006; Wiseman *et al*.;2007). Bone morphogenic protein 7 (BMP-7) plays an important role in the initiation and development of tumor, and also promotes its progression (Thawani *et al*.; 2010). The low expression of BMP-7 protein during carcinogenesis, in several human tumors, contributes to bone metastases. Furthermore, according to the results of our EMT screening, BMP-7 has been shown to inhibit the proliferation of ATC cells through the over-expression of p21 and p27 (Franzen *et al*.; 2001).

In particular, among the genes more deregulated in ATC, I chose to focus my work on JAM-A.

The adhesion protein JAM-A is a transmembrane protein located in the tight junctions of endothelial and epithelial cells where it promotes cell-cell adhesion. JAM-A belongs to the immunoglobulin (Ig) superfamily, and previous studies have shown that JAM-A also plays a role in other cellular processes, such as leukocyte migration, platelet activation and angiogenesis.

Other data in the literature suggest that EMT is involved in the passage from PTC cells to ATC cells, and for this reason JAM-A could be considered a marker for the evolution of the thyroid tumor in the anaplastic form.

JAM-A is overexpressed in some cancers and under-expressed in others, and this behavior could be in part also explained by its structure. The protein has a cytoplasmic tail that does not have catalytic activity but contains a class II PDZ binding domain that is present at the C terminal of the protein, and which interacts with different proteins (Songyang *et al*.; 1997). The type of interaction between JAM-A and other proteins could lead to either a promotion or an inhibition of the tumorigenesis markers. On the other hand, the mechanisms that lead to an altered expression of JAM-A in tumors are still unclear: it is possible that the regulation mechanism of JAM-A and the role of this protein depend on the cellular background. There are some hypotheses that could explain the loss of this protein in ATC. JAM-A is implicated in carcinogenesis through various signaling pathways such as

that of TGF-β1 (Zhao *et al.*;2014). For example, TGF-β1-mediated signaling induces under-expression of JAM-A in breast cancer, with an increase of the invasive capacity of cancer cells (Wang *et al.*; 2012). Activation of the signaling pathway mediated by TGF-β1 is also important in ATC (Sun *et al.*;2017; Knauf *et al.*;2011). Furthermore, the expression of JAM-A can be regulated by pro-inflammatory cytokines, such as TNF-α and IFN-$_{\gamma}$, which are also involved in the progression of thyroid cancer (Jaczewska, *et al.*; 2014; Dossus *et al.*; 2018). In fact, the correlation between inflammation and thyroid cancer is well known. Thyroid cancers are often infiltrated by dendritic cells, mast cells and macrophages. It has also been seen that ATC contains more than 50% of tumor associated macrophages (TAM) (Hèbrant *et al.*;2014). In patients with thyroid cancer there is also a relationship between the increase of TAMs number and a decrease of survival in these patients. In one study it was observed that in chronic inflammations and in autoimmune thyroid diseases, such as Hashimoto's thyroiditis (TH), there is an increase in the incidence of thyroid cancer. Interestingly, it has also been observed that thyroid cells in TH's patients present a loss of epithelial integrity and a significant reduction in the expression of tight junction proteins (ZO-1, Claudine and JAM-A) (Rebuffat *et al.*; 2013). These data would suggest that inflammation in thyroid cancer may be responsible for the reduced expression of JAM-A.

The loss of JAM-A could therefore be due to inflammation in the microenvironment created by the tumor, and represents a link between inflammation and thyroid carcinoma.

Here we have shown that the over-expression of JAM-A activates p53: this could be one of the mechanism behind the inhibition of ATC cell proliferation. P53 is a tumor suppressor frequently mutated in many human carcinomas that plays a very important role in genomic stability and its activation is a primary mechanism which occurs following pathological responses to DNA damage by agents such as chemotherapy and radiation therapy. The proteins encoded by the TP53 gene bind to DNA regulating gene expression and preventing mutation in the genome. Mutations in this gene obviously lead to uncontrolled cell division. More than 50% of human cancers have been shown to

contain a mutation or deletion of the p53 gene, and mutations in p53 are characteristic of poorly differentiated or anaplastic thyroid carcinomas (Liu *et al*; 2017).

We also observed that JAM-A induces GSK3 α / β phosphorylation on serine 9 and serine 21 respectively. GSK3 α / β is a serine-threonine kinase implicated in several signaling pathways, such as the one which regulates the amount of glucose, cell proliferation and migration. In the past GSK3 α / β has been evaluated as a possible target for the suppression of inflammation in neurodegenerative diseases such as Alzhaimer, and in addition today there is a lot of interest in developing GSK3 α / β inhibitors for use in antineoplastic therapy (Beurel *et al*.; 2015; Morales *et al.*; 2014). Changes at GSK3 α / β level influence its enzymatic activity and therefore the regulation of the signal transduction pathways downstream of this protein. In particular, the phosphorylation of GSK3 α / β on Serine 21 and Serine 9, via kinases such as AKT (Cross *et al*.; 1995) and PKA (Fang *et al*.; 2000), is an inhibitory mechanism which prevent GSK3 α / β to bind its substrates (Schrecengost *et al*.; 2018).

In summary, JAM-A could be a new marker of thyroid tumor progression, and in the future it could be supposed that by restoring the expression of this protein, a potential therapeutic effect can be obtained in the treatment of ATC, not only in a direct way through JAM-A, but also by acting on the mechanisms downstream of its signaling pathway, such as those mediated by the tumor suppressor p53 and the enzyme GSK3 α / β.

CONCLUSIONS

One of the important question is to understand the mechanisms of thyroid tumor progression.

Anaplastic thyroid carcinoma represents the rarest of all thyroid cancers, but it is responsible for about 50% of thyroid cancer mortality. In this dissertation work, I aim to identify new biomarker of ATC for the development of novel treatments. In detail a focused on two proteins that have a tumor suppressor effects in thyroid carcinogenesis.

In Summary my work showed that the ectopic expression of TUSC2 in thyroid cancer cell lines reduces cell proliferation, migration and invasion. In part the effects are mediated by SMAC/DIABLO protein. These findings could imply the possibility that restoration of TUSC2 expression, could be used in the therapy of aggressive thyroid cancer.

Finally, in my PhD studies I have individuated JAM-A as a novel marker of EMT in thyroid tumor progression. The work which I contributed, demonstrated that JAM-A is down-regulated in ATC and that the restoration of its expression suppressed malignant hallmarks of transformation including proliferation and motility. For this reason, JAM-A restoration might have a therapeutic potential in the treatment of ATC.

In conclusion, I identified new molecular markers implicated in cell motility and proliferation that could be used in the diagnosis and therapy of aggressive form of thyroid cancer.

MATERIALS AND METHODS

1. Tissue samples

Tumors and normal thyroid tissue samples for RNA extraction, quantitative RT-PCR and immunohistochemistry analysis were retrieved from the files of the Department of Surgery, University of Pisa (Italy). Processing of samples and of patient information proceeded in agreement with the principles of the Helsinki Declaration of 1975.

2. Immunohistochemistry

For immunohistochemistry analysis, in collaboration with Prof. F. Basolo, University of Pisa, we analyzed 48 ATC samples, 14 PTC of the classic variant and 19 normal tissue distant from neoplasia or from contralateral lobe. Tissue from colon adenocarcinoma was used as positive control. All samples were fixed in formalin-fixed and paraffin-embedded (FFPE). The slides of tumor sections were incubated with a rabbit polyclonal antibody against JAM-A (JAM1/CD31, Thermo Fisher Scientific) and processed according to standard procedures. Cases were scored as positive when cytoplasmic staining was observed in tumor cells. Immunoreactivity was expressed as the percentage of positively stained cells.

3. Quantitative Real-time PCR (q-RT-PCR)

RNA was isolated using the mirVanaTM miRNA Isolation Kit (Thermo Scientific, Waltham, MA, USA) according to the manufacturer's instructions. The purity and quantity of RNA were assessed using the NanoDrop spectrophotometer (Thermo Scientific, Wilmington, DE, USA). The quality of the RNAs was verified by the 2100 Bioanalyzer (Agilent Techonologies, Waldbronn, Germany). Only samples with RNA integrity number (RIN) value > 7 were used for further analysis.

To evaluated the mRNA expression levels, 1 μg was reversed with the QuantiTect Reverse Transcription (Qiagen, Crawley, UK) according to manufacturer's instructions. The expression levels of mRNA were measured by q-RT-PCR using specific primer and TaqMan Universal PCR Master Mix (Thermo Scientific, Waltham, MA, USA). β-actin was used as an endogenous control. PCR reactions were performed in triplicate and fold changes were calculated with the formula: 2-(sample 1 ΔCt - sample 2 ΔCt).

4. Cell cultures

The anaplastic thyroid cancer cells lines CAL62, 8505C and the human papillary thyroid cancer cells, TPC-1 (named TPC) were grown in Dulbecco's modified Eagle's medium (DMEM) (Thermo Fisher Scientific, Walthman, MA, USA). The normal immortalized human primary thyroid follicular epithelial cell line (Nthy-ori 3-1) was grown in Roswell Park Memorial Institute 1640 (RPMI). All growth media used containing 10% FBS (fetal bovine serum), L-glutamine and penicillin/streptomycin (Invitrogen, Carlsbad, CA, USA).

5. Plasmids

The plasmids were obtained from Gene Copeia (Rockville, MD, USA):

- TUSC2 plasmid and relative control named CMV;

- JAM-A plasmid control; sh-JAM-A plasmide and relative control named

- SMAC/DIABLO (EX-U1000-M43).

6. Transfection

For stable transfection, CAL62, 8505C and TPC-1 cells (1×10^5) cells were transfected with Lipofectamine 2000 (Thermo Scientific) and 4 µg of plasmid according the manufacturer's instructions. 48 hours after transfection, several mass populations and cell clones were selected with puromycin (Sigma-Aldrich, St. Louis, MO, USA). The cells transfected with TUSC2 were selected with geneticin (Sigma-Aldrich, St. Louis, MO, USA). The efficiency of transfection for expression of TUSC2 and JAM-A were analyzed by Western blot. A mass population of each generated line was used for successive experiments.

8505C/TUSC2 and 8505C/C.vector were transiently transfected with the specific small interfering RNAs (siRNAs) for SMAC/DIABLO named SMAC-5 (catalogue number SI02655576) and SMAC-6 (catalogue number SI00299999) (QIAGEN) in 6-well plates in triplicate.

Finally for transiently transfection of Nthy-ori 3-1, the cells were transfected with 5 µl of 100 µM of small interfering RNA (FlexiTube siRNA Qiagen, Hilden, Germany) specific for TUSC2 named TUSC2-5 (Catalog number SI02664606) and TUSC2-6 (Catalog number SI0266461), and with a negative control siRNA (AllStars Negative Control siRNA; SI03650318). All transient transfection were performed using HiPerFect Transfection (Qiagen) reagent, according to the manufacturer's protocol.

7.Immunoblotting

For Western blot analysis cell lines were lysed in JS Buffer followed by centrifugation at 13,000 rpm at 4°C for 30 minutes. Protein concentration was determined using Bradford assay (Bio-Rad, Munich, Germany) and separated on polyacrylamide SDS-PAGE and transferred to nitrocellulose membranes. The membranes were incubated with primary antibody overnight at 4°C:

-mouse monoclonal anti-α Tubulin, 1:10000 (Sigma-Aldrich);

-rabbit polyclonal anti-TUSC2 1:200 (Abcam, Cambridge, UK);

-mouse monoclonal anti-SMAC/DIABLO, 1:1000 (Cell signaling, Danvers, MA)

-mouse monoclonal anti CYTOCHROME C, 1:500 (Santa Cruz, Dallas, USA)

-rabbit monoclonal anti-p21, 1:1000 (Cell Signaling)

- rabbit monoclonal anti-p27, 1:1000 (Cell Signaling)

- mouse monoclonal anti-CDK6, 1:1000 (Cell Signaling)

- anti-JAM-A 1:500 (Santa Cruz)

- anti GSK3 α/β phosphorylated 1: 1000 (Cell Signaling Technology)

- anti-p53 phosphorylated 1: 1000 (Cell Signaling Technology)

Secondary anti-mouse and anti-rabbit antibody, conjugated to horseradish peroxidase, were purched from Bio-Rad (Hercules, CA) and diluted 1:3000. For detection of the band signal intensity enhanced chemiluminescence detection kit was used (ECL Thermo Fisher Scientific).

8. Array

Proteome Profiler Human Phospho-Kinase Array Kit (R&D Systems, Minneapolis, MN, USA) was used to analyze the phosphorylated proteins.

Cells were lysate and added (500 ng) to the membranes of the array spotted with antibodies directed towards different phosphorylated proteins. The spots, were obtained after autoradiographic exposure and quantized using ImageJ 1.38e software.

For Human Apoptosis array, cells were treated with 2.5 µM of staurosporin for 24 hours. At the end of the treatment the cells were lysed with the Lysis Buffer and quantized with the Bradford method. Cell lysate were resuspended in 100 and then were hybridized with the array membrane Proteome Profiler Human Apoptosis Array Kit (R&D Systems, Minneapolis, MN). Plot were detected with Chemi Reagent Mix and the image were acquired, in duplicate, through autoradiographic exposure. Quantification of array was performed with the Image J software programe (version 1.50i).

9. Cell proliferation assay

For cell proliferation curves, 3x 10^4 thyroid cell lines were plated in a 6 well plates and counted in triplicate every 24 hours for 4 days with TC10 automated cell counter (Bio-Rad).

8505C cell transfected with TUSC2 plasmid and relative control, was determined cell viability by MTS-assay (CellTiter 96® AQueous One Solution Assay, Promega, WI, USA). Briefly, 1x103 cells were plated in triplicate into 96-well culture plates. 20 µl of MTS solution were added to each well for 30 minutes after 24, 48, 72 h and after seventh day. The quantity of formazan produced was determined by measuring absorbance at 490 nm using Microplated reader (Model 550, Ultramark Microplate Reader, Bio-Rad).

We performed a colony formation assay on CAL62 cells after transfection with JAM-A or with the control plasmid. After 14 days the colonies formation were fixed and stained with crystal violet for ten minutes. Finally, the colonies were photographed and counted.

10. Trypan blue assay

For trypan blue assay transfected cells were plated in a 6-well plate. After day, cells were treated with 1 µM doxorubicin (Sigma-Aldrich) for 48 hours and with 2.5 µM staurosporine (Sigma-Aldrich) for 24 hours. After treatment, cells were trypsinized, stained with 0.4% trypan blue reagent (Bio-Rad). The count was performed in triplicate using TC20^{TM} Automated Cell Counter (Bio-Rad). Cell viability was expressed in percentage and was calculated by dividing the number of unstained (viable) cells by the number of total cells (stained and unstained).

11. Flow cytometry

Fluorescence-activated cell sorting (FACS) analysis was performed to evaluated cell cycle progression and cell death. To this aim was used using propidium iodide staining and an FC500 Cytometer (Beckman Coulter, Milan, Italy).

For the cell cycle progression, cells were stained with the DNA PREP Reagents Kit (Beckman Coulter) according to the manufacturer's instructions, and a minimum of 10,000 single cell events were recorded using the CXP Software (Beckman Coulter). Finally, cell cycle analysis was performed using Kaluza Analysis Software 2.1 (Beckman Coulter) with the Michael Fox algorithm to determine G1, S and G2/M phases.

For cell death, cells were treated with staurosporine (2.5 μM) for 6 h and incubated with 1 μl of a 10 μg/mL propidium iodide (PI) solution (Beckman Coulter) for FACS analysis.

12. Migration assay

Wound healing was performed to evaluate cell migration ability.

For wound healing assay, $5x10^5$ cells were seeded in a 6-well culture plates and after day a scratch was inflicted on confluent monolayer cells. The closure of scrape area was monitored and photographed. The wound area was measured through Cell[a] software (Olympus Biosystem GmbH) and expressed as percentage of wound closure respect to control cells.

13. Invasion assay

Cell invasion was examined using a reconstituted extracellular matrix (Matrigel, BD Biosciences, San Jose, CA). The cell suspension (1 x 105 cells for well) was resuspended in serum free culture medium (100 μl) and loaded onto the upper chamber of Transwell cell culture chambers on a prehydrated polycarbonate membrane filter of 8-μm pore size (Costar, Cambridge, MA) coated with 35 μg of Matrigel (BD Biosciences, San Jose, CA). The lower chamber was filled with 2.5% medium

(500 µl). After 24-h incubation at 37°C, non-migrating cells on the upper side of the filter were wiped-off. Invading cells were stained with glutaraldehyde 11% (Sigma-Aldrich, St. Louis, MO, USA) for 90 minutes. Subsequently the upper chamber were colored with crystal violet and quantified at OD 570 nm after color extraction, in triplicate.

14. Colony formation assay

Cell lines were transfected with Lipofectamine 2000 and relative plasmids. After 48 hours from transfection, cells were selected with Puromycin and later 14 days the colonies were stained with a 0.5% Crystal Violet solution (containing methanol and deionized water in a 1: 5 dilution) for 10 minutes. Finally, the colonies were photographed and counted.

15. Trans-endothelial migration assay

For trans-endhothelial migration, $5x10^4$ CAL62/ JAM-A and CAL62 transfected with empty vector were seeded on a Transwell insert with 8-µm pores (Cell Biolabs, San Diego, CA) coated with a monolayer of human umbilical vein endothelial cells (HUVECs) cells. after 48 hours of incubation at 37° C, cells that invaded monolayer were colored with crystal violet, photographed and quantification as absorbance at O.D 550 nm.

16. Statistical analyses

All results were represented as the means and standard deviation (mean ± SD) Statistical analyzes was elaborated with the GraphPad Prism 6 software (GraphPad Software, La Jolla, California, USA). Values were considered statistically significant when $p < 0.05$.

REFERENCES

Abdullah MI, Junit SM, Ng KL, Jayapalan JJ, Karikalan B, Hashim OH. Papillary Thyroid Cancer: Genetic Alterations and Molecular Biomarker Investigations. Int J Med Sci. 2019 Feb 28;16(3):450-460. PubMed PMID: 30911279 doi: 10.7150/ijms.29935

Acquaviva G, Visani M, Repaci A, Rhoden KJ, de Biase D, Pession A, Giovanni T. Molecular pathology of thyroid tumours of follicular cells: a review of genetic alterations and their clinicopathological relevance. Histopathology. 2018 Jan;72(1):6-31. PubMed PMID: 29239040 doi: 10.1111/his.13380

Aratake Y, Nomura H, Kotani T, Marutsuka K, Kobayashi K, Kuma K, Miyauchi A, Okayama A, Tamura K. Coexistent anaplastic and differentiated thyroid carcinoma. Am J Clin Pathol. 2006. Mar;125(3):399-406. doi: 10.1309/lf3q-1nqk-mt2n-9knv.PMID: 16613808

Aurrand-Lions MA, Duncan L, Pasquier LD, Imhof BA. Cloning of JAM-2 and JAM3: an emerging junctional adhesion molecular family? Curr Top Microbiol Immunol. 2000. PMID: 11036763 doi: 10.1007/978-3-642-57276-0_1

Beurel E, Grieco SF, Jope RS. Glycogen synthase kinase-3 (GSK3): regulation, actions, and diseases. Pharmacology & therapeutics. 2015 Apr;148:114-31. PMID: 25435019 doi: 10.1016/j.pharmthera.2014.11.016.

Bible KC, Ryder M. Evolving molecularly targeted therapies for advanced-stage thyroid cancers. Nat Rev Clin Oncol. 2016 Jul;13(7):403-16. Doi 10.1038/nrclinonc.2016.19. Epub 2016 Mar 1. Review. PubMed PMID: 26925962.

Brabletz T., Kalluri R., Nieto MA e Weinberg RA. EMT in cancer. 2018 February. Nature Review Cancer 18(2):128-1 doi: 10.1038/nrc.2017.118. Epub 2018 Jan 12.

Brose MS, Cabanillas ME, Cohen EE, et al. Vemurafenib in patients with BRAF(V600E)-positive metastatic or unresectable papillary thyroid cancer refractory to radioactive iodine: a non-randomised, multicentre, open-label, phase 2 trial. Lancet Oncology 2016;17(9):1272–82.

Cabanillas ME, McFadden DG, Durante C. Thyroid cancer. Lancet. 2016 Dec 3;388(10061):2783-2795. doi: 10.1016/S0140-6736(16)30172-6. Epub 2016 May 27 Review. PubMed PMID: 27240885

Cancer Genome Atlas Research Network. Integrated genomic characterization of papillary thyroid carcinoma.Cell. 2014 Oct 23;159(3):676-90. doi: 10.1016/j.cell.2014.09.050.

Celano M, Rosignolo F, Maggisano V, Pecce V, Iannone M, Russo D, Bulotta S.MicroRNAs as Biomarkers in Thyroid Carcinoma. Int J Genomics. 2017;2017:6496570. doi: 10.1155/2017/6496570. Epub 2017 Sep 6. Review. PubMed PMID: 29038786; PubMed Central PMCID: PMC5606057

Ceolin L, Duval MADS, Benini AF, Ferreira CV, Maia AL. Medullary thyroid carcinoma beyond surgery: advances, challenges, and perspectives. Endocr Relat Cancer. 2019 Aug 1;26(9):R499-R518. doi: 10.1530/ERC-18-0574

Cross DA, Alessi DR, Cohen P, Andjelkovich M, Hemmings BA. Inhibition of glycogen synthase kinase-3 by insulin mediated by protein kinase B. Nature. 1995 Dec 21-28;378(6559):785-9. doi: 10.1038/378785a0..

Dai B., Yan S., Lara-Guerra H., Kawashima H., Sakai R., Jayachandran G., Majidi M., Mehran R., Wang J., Bekele B.N., et al. Exogenous Restoration of TUSC2 Expression Induces Responsiveness to Erlotinib in Wildtype Epidermal Growth Factor Receptor (EGFR) Lung Cancer Cells through Context Specific Pathways Resulting in Enhanced Therapeutic Efficacy. PLoS ONE. 2015;10:e0123967. doi: 10.1371/journal.pone.0123967

Deng WG, Wu G, Ueda K, Xu K, Roth JA, Ji L. Enhancement of antitumor activity of cisplatin in human lung cancer cells by tumor suppressor FUS1. Cancer Gene Therapy 2008 Jan;15(1):29-39. doi: 10.1038/sj.cgt.7701094.

DeLellis RA, Lloyd RV, Heitz PU, Eng C, editors. Pathology and Genetics of Tumors of the Endocrine Organs. Lyon: IARC Press; 2004.

Du L, Schageman JJ, Subauste MC, Saber B, Hammond SM, Prudkin L, Wistuba Ii, Ji L, Roth JA, Minna JD, Pertsemlidis A. miR-93, miR-98, and miR-197 regulate expression of tumor suppressor gene FUS1. Mol Cancer Res. 2009; 7(8):1234–1243.

Dossus L, Franceschi S, Biessy C, Navionis AS, Travis RC, Weiderpass E, Scalbert A, Romieu I, Tjønneland A, Olsen A, Overvad K, Boutron-Ruault MC, Bonnet F, Fournier A, Fortner RT, Kaaks R, Aleksandrova K, Trichopoulou A, La Vecchia C,Peppa E, Tumino R, Panico S, Palli D, Agnoli C, Vineis P, Bueno-de-Mesquita HBA, Peeters PH, Skeie G, Zamora-Ros R, Chirlaque MD, Ardanaz E, Sánchez MJ, Ramón Quirós J, Dorronsoro M, Sandström M, Nilsson LM, Schmidt JA, Khaw KT, Tsilidis KK, Aune D, Riboli E, Rinaldi S. Adipokines and inflammation markers and risk of differentiated thyroid carcinoma: The EPIC study. Int J Cancer. 2018 Apr 1;142(7):1332-1342. doi: 10.1002/ijc.31172 PMID: 29168186.

Durante C, Grani G, Lamartina L, Filetti S, Mandel SJ, Cooper DS. The Diagnosis and Management of Thyroid Nodules: A Review. JAMA. 2018 Mar 6;319(9):914-924. doi: 10.1001/jama.2018.0898. Review. Erratum in: JAMA. 2018 Apr 17;319(15):1622. PubMed PMID: 29509871.

Fagin JA, Wells SA Jr. Biologic and Clinical Perspectives on Thyroid Cancer. N Engl J Med. 2016 Sep 15;375(11):1054-67. doi: 10.1056/NEJMra1501993.Review.PubMed PMID: 27626519; PubMed Central PMCID: PMC5512163.

Fang X, Yu SX, Lu Y, Bast RC Jr, Woodgett JR, Mills GB. Phosphorylation and inactivation of glycogen synthase kinase 3 by protein kinase A. Proc Natl Acad Sci U S A. 2000 Oct 24;97(22):11960-5. PubMed PMID: 11035810; PubMed Central PMCID: PMC17277.

Filetti S, Durante C, Hartl D, Leboulleux S, Locati LD, Newbold K, Papotti MG,Berruti A; ESMO Guidelines Committee. Electronic address: clinicalguidelines@esmo.org. Thyroid cancer: ESMO Clinical Practice Guidelines for diagnosis, treatment and follow-up. Ann Oncol. 2019 Dec 1;30(12):1856-1883. doi: 10.1093/annonc/mdz400. PubMed PMID: 31549998.

Fong D, Spizzo G, Mitterer M, Seeber A, Steurer M, Gastl G, Brosch I, Moser P. Low expression of junctional adhesion molecule A is associated with metastasis and poor survival in pancreatic cancer. Ann Surg Oncol. 2012 Dec;19(13):4330-6.doi: 10.1245/s10434-012-2381-8. Epub 2012 May 2. PubMed PMID: 22549289.

Franzén A, Heldin NE. BMP-7-induced cell cycle arrest of anaplastic thyroid carcinoma cells via p21(CIP1) and p27(KIP1). Biochem Biophys Res Commun. 2001 Jul 20;285(3):773-81. PubMed PMID: 11453659.

Fugazzola L, Elisei R, Fuhrer D, Jarzab B, Leboulleux S, Newbold K, Smit J.2019 European Thyroid Association Guidelines for the Treatment and Follow-Up of Advanced Radioiodine-Refractory Thyroid Cancer. Eur Thyroid J. 2019 Oct;8(5):227-245. doi: 10.1159/000502229. Epub 2019 Aug 28. Review. PubMed PMID:31768334; PubMed Central PMCID: PMC6873012.

Fuziwara CS, Kimura ET. MicroRNA Deregulation in Anaplastic Thyroid Cancer Biology. Int J Endocrinol. 2014;2014:743450. doi: 10.1155/2014/743450. Epub 2014 Aug 19. Review. PubMed PMID: 25202329; PubMed Central PMCID: PMC4151544.

Ganly I, Makarov V, Deraje S, Dong Y, Reznik E, Seshan V, Nanjangud G, Eng S, Bose P, Kuo F, Morris LGT, Landa I, Carrillo Albornoz PB, Riaz N, Nikiforov YE, Patel K, Umbricht C, Zeiger M, Kebebew E, Sherman E, Ghossein R, Fagin JA, Chan TA. Integrated Genomic Analysis of Hürthle Cell Cancer Reveals Oncogenic Drivers,Recurrent Mitochondrial Mutations, and Unique Chromosomal Landscapes. Cancer Cell. 2018 Aug 13;34(2):256-270.e5. doi: 10.1016/j.ccell.2018.07.002. PubMed PMID: 30107176; PubMed Central PMCID: PMC6247912.

Giacinti C, Giordano A. RB and cell cycle progression. Oncogene. 2006 Aug 28;25(38):5220-7. Review. PubMed PMID: 16936740.

González-Mariscal L, Lechuga S, Garay E. Role of tight junctions in cell proliferation and cancer. Prog Histochem Cytochem. 2007;42(1):1-57. Epub 2007 Feb 27.Review. PubMed PMID: 17502225.

Gopal RK, Kübler K, Calvo SE, Polak P, Livitz D, Rosebrock D, Sadow PM, Campbell B, Donovan SE, Amin S, Gigliotti BJ, Grabarek Z, Hess JM, Stewart C, Braunstein LZ, Arndt PF, Mordecai S, Shih AR, Chaves F, Zhan T, Lubitz CC, Kim J,Iafrate AJ, Wirth L, Parangi S, Leshchiner I, Daniels GH, Mootha VK, Dias-Santagata D, Getz G, McFadden DG. Widespread Chromosomal Losses and Mitochondrial DNA Alterations as Genetic Drivers in Hürthle Cell Carcinoma Cancer Cell. 2018 Aug 13;34(2):242-255.e5. doi: 10.1016/j.ccell.2018.06.013.PubMed PMID: 30107175; PubMed Central PMCID: PMC6121811.

Guo Z, Hardin H, Montemayor-Garcia C, Asioli S, Righi A, Maletta F, Sapino A, Lloyd RV. In Situ Hybridization Analysis of miR-146b-5p and miR-21 in Thyroid Nodules: Diagnostic Implications. Endocr Pathol. 2015 May;26(2):157-63. doi:10.1007/s12022-015-9363-x. PubMed PMID: 25771986.

Gutwein P, Schramme A, Voss B, Abdel-Bakky MS, Doberstein K, Ludwig A, Altevogt P, Hansmann ML, Moch H, Kristiansen G, Pfeilschifter J. Downregulation of junctional adhesion molecule-A is involved in the progression of clear cell renal cell carcinoma. Biochem Biophys Res Commun. 2009 Mar 6;380(2):387-91. doi: 10.1016/j.bbrc.2009.01.100. Epub 2009 Jan 23. PubMed PMID: 19250634.

Haddad RI, Lydiatt WM, Ball DW, Busaidy NL, Byrd D, Callender G, Dickson P,Duh QY, Ehya H, Haymart M, Hoh C, Hunt JP, Iagaru A, Kandeel F, Kopp P, Lamonica DM, McCaffrey JC, Moley JF, Parks L, Raeburn CD, Ridge JA, Ringel MD, Scheri RP,Shah JP, Smallridge RC, Sturgeon C, Wang TN, Wirth LJ, Hoffmann KG, Hughes M. Anaplastic Thyroid Carcinoma, Version 2.2015. J Natl Compr Canc Netw. 2015 Sep;13(9):1140-50. PubMed PMID: 26358798; PubMed Central PMCID: PMC4986600.

Haroon Al Rasheed MR, Xu B. Molecular Alterations in Thyroid Carcinoma. Surg Pathol Clin. 2019 Dec;12(4):921-930. doi: 10.1016/j.path.2019.08.002. Epub 2019 Sep 27. Review. PubMed PMID: 31672298; PubMed Central PMCID: PMC6883923.

He H, Jazdzewski K, Li W, Liyanarachchi S, Nagy R, Volinia S, Calin GA, Liu CG, Franssila K, Suster S, Kloos RT, Croce CM, de la Chapelle A. The role of microRNA genes in papillary thyroid carcinoma. Proc Natl Acad Sci U S A. 2005 Dec 27;102(52):19075-80. Epub 2005 Dec 19. PubMed PMID: 16365291; PubMed Central PMCID: PMC1323209.

Hébrant A, Floor S, Saiselet M, Antoniou A, Desbuleux A, Snyers B, La C, de Saint Aubain N, Leteurtre E, Andry G, Maenhaut C. miRNA expression in anaplastic thyroid carcinomas. PLoS One. 2014 Aug

25;9(8):e103871. doi:10.1371/journal.pone.0103871. eCollection 2014. PubMed PMID: 25153510; PubMed Central PMCID: PMC4143225.

Howell GM, Hodak SP, Yip L. RAS mutations in thyroid cancer. Oncologist.2013;18(8):926-32. doi: 10.1634/theoncologist.2013-0072. Epub 2013 Jul 19.Review. PubMed PMID: 23873720; PubMed Central PMCID: PMC3755930.

Huang JY, Xu YY, Sun Z, Wang ZN, Zhu Z, Song YX, Luo Y, Zhang X, Xu HM. Low junctional adhesion molecule A expression correlates with poor prognosis in gastric cancer. J Surg Res. 2014 Dec;192(2):494-502. doi:10.1016/j.jss.2014.06.025. Epub 2014 Jun 18. PubMed PMID: 25033702.

Ivanova AV, Ivanov SV, Pascal V, Lumsden JM, Ward JM, Morris N, Tessarolo L,Anderson SK, Lerman MI. Autoimmunity, spontaneous tumourigenesis, and IL-15 insufficiency in mice with a targeted disruption of the tumour suppressor gene Fus1.J Pathol. 2007 Apr;211(5):591-601. PubMed PMID: 17318811.

Ivanova AV, Ivanov SV, Prudkin L, Nonaka D, Liu Z, Tsao A, Wistuba I, Roth J,Pass HI. Mechanisms of FUS1/TUSC2 deficiency in mesothelioma and its tumorigenic transcriptional effects. Mol Cancer. 2009 Oct 24;8:91. doi:10.1186/1476-4598-8-91. PubMed PMID: 19852844; PubMed Central PMCID: PMC2776015.

Jaczewska J, Abdulreda MH, Yau CY, Schmitt MM, Schubert I, Berggren PO, Weber C, Koenen RR, Moy VT, Wojcikiewicz EP. TNF-α and IFN-γ promote lymphocyte adhesion to endothelial junctional regions facilitating transendothelial migration. J Leukoc Biol. 2014 Feb;95(2):265-74. doi: 10.1189/jlb.0412205. Epub 2013 Sep 26. PubMed PMID: 24072879; PubMed Central PMCID: PMC3896659.

Jayarangaiah A, Sidhu G, Brown J, Barrett-Campbell O, Bahtiyar G, Youssef I, Arora S, Skwiersky S, McFarlane SI. Therapeutic options for advanced thyroid cancer. Int J Clin Endocrinol Metab. 2019;5(1):26-34. doi: 10.17352/ijcem.000040.Epub 2019 Sep 9. PubMed PMID: 31709422; PubMed Central PMCID: PMC6839707.

Ji L, Minna JD, Roth JA. 3p21.3 tumor suppressor cluster: prospects for translational applications. Future Oncol. 2005 Feb;1(1):79-92. Review. PubMed PMID: 16555978.

Kakuki T, Kurose M, Takano K, Kondoh A, Obata K, Nomura K, Miyata R, Kaneko Y,Konno T, Takahashi S, Hatakeyama T, Kohno T, Himi T, Kojima T. Dysregulation of junctional adhesion molecule-A via p63/GATA-3 in head and neck squamous cell carcinoma. Oncotarget. 2016 Jun 7;7(23):33887-900. doi: 10.18632/oncotarget.8432.PubMed PMID: 27036044; PubMed Central PMCID: PMC5085126.

Keiper T, Santoso S, Nawroth PP, Orlova V, Chavakis T. The role of junctional adhesion molecules in cell-cell interactions. Histol Histopathol. 2005 Jan;20(1):197-203. doi: 10.14670/HH-20.197. Review. PubMed PMID: 15578438.

Kelly LM, Barila G, Liu P, Evdokimova VN, Trivedi S, Panebianco F, Gandhi M,Carty SE, Hodak SP, Luo J, Dacic S, Yu YP, Nikiforova MN, Ferris RL, Altschuler DL, Nikiforov YE. Identification of the transforming STRN-ALK fusion as a potential therapeutic target in the aggressive forms of thyroid cancer. Proc Natl Acad Sci U S A. 2014 Mar 18;111(11):4233-8. doi:10.1073/pnas.1321937111. Epub 2014 Feb 3. PubMed PMID: 24613930; PubMed Central PMCID: PMC3964116.

Kim J, Gosnell JE, Roman SA. Geographic influences in the global rise of thyroid cancer. Nat Rev Endocrinol. 2020 Jan;16(1):17-29. doi: 10.1038/s41574-019-0263-x. Epub 2019 Oct 15. Review. PubMed PMID: 31616074.

Kitahara CM, Sosa JA. The changing incidence of thyroid cancer. Nat Rev Endocrinol. 2016 Nov;12(11):646-653. doi: 10.1038/nrendo.2016.110. Epub 2016 Jul 15. Review. PubMed PMID: 27418023.

Knauf JA, Sartor MA, Medvedovic M, Lundsmith E, Ryder M, Salzano M, Nikiforov YE, Giordano TJ, Ghossein RA, Fagin JA. Progression of BRAF-induced thyroid cancer is associated with epithelial-mesenchymal transition requiring concomitant MAP kinase and TGFβ signaling. Oncogene. 2011 Jul 14;30(28):3153-62. doi:10.1038/onc.2011.44. Epub 2011 Mar 7. PubMed PMID: 21383698; PubMed CentralPMCID: PMC3136543.

Landa I, Ibrahimpasic T, Boucai L, Sinha R, Knauf JA, Shah RH, Dogan S, Ricarte-Filho JC, Krishnamoorthy GP, Xu B, Schultz N, Berger MF, Sander C, Taylor BS, Ghossein R, Ganly I, Fagin JA. Genomic and transcriptomic hallmarks of poorly differentiated and anaplastic thyroid cancers. J Clin Invest. 2016 Mar 1;126(3):1052-66. doi: 10.1172/JCI85271. Epub 2016 Feb 15. PubMed PMID: 26878173;PubMed Central PMCID: PMC4767360.

Lee DY, Deng Z, Wang CH, Yang BB. MicroRNA-378 promotes cell survival, tumor growth, and angiogenesis by targeting SuFu and Fus-1 expression. Proc Natl Acad Sci U S A. 2007 Dec 18;104(51):20350-5. Epub 2007 Dec 11. PubMed PMID: 18077375; PubMed Central PMCID: PMC2154434.

Lee HJ, Lee WK, Kang CW, Ku CR, Cho YH, Lee EJ. A selective cyclin-dependent kinase 4, 6 dual inhibitor, Ribociclib (LEE011) inhibits cell proliferation and induces apoptosis in aggressive thyroid cancer. Cancer Lett. 2018 Mar 28;417:131-140. doi: 10.1016/j.canlet.2017.12.037. Epub 2018 Jan 4. PubMed PMID: 29306020.

Lerman MI, Minna JD. The 630-kb lung cancer homozygous deletion region on human chromosome 3p21.3: identification and evaluation of the resident candidate tumor suppressor genes. The International Lung Cancer Chromosome 3p21.3 Tumor Suppressor Gene Consortium. Cancer Res. 2000 Nov 1;60(21):6116-33. PubMed PMID:11085536.

Liang S, Zhang N, Deng Y, Chen L, Zhang Y, Zheng Z, Luo W, Lv Z, Li S, Xu T. miR-663b promotes tumor cell proliferation, migration and invasion in nasopharyngeal carcinoma through targeting TUSC2. Exp Ther Med. 2017 Aug;14(2):1095-1103. doi: 10.3892/etm.2017.4608. Epub 2017 Jun 14. PubMed PMID: 28781619; PubMed Central PMCID: PMC5526187.

Li G, Kawashima H, Ji L, Ogose A, Ariizumi T, Umezu H, Xu Y, Hotta T, Endo N.Frequent absence of tumor suppressor FUS1 protein expression in human bone and soft tissue sarcomas. Anticancer Res. 2011 Jan;31(1):11-21. PubMed PMID:21273575.

Li L, Yu C, Ren J, Ye S, Ou W, Wang Y, Yang W, Zhong G, Chen X, Shi H, Su X,Chen L, Zhu W. Synergistic effects of eukaryotic coexpression plasmid carrying LKB1 and FUS1 genes on lung cancer in vitro and in vivo. J Cancer Res Clin Oncol.2014 Jun;140(6):895-907. PubMed PMID: 24659339.

Liu L, Li D, Chen Z, Yang J, Ma Y, Cai H, Shan C, Lv Z, Zhang X. Wild-Type P53Induces Sodium/Iodide Symporter Expression Allowing Radioiodide Therapy in Anaplastic Thyroid Cancer. Cell Physiol Biochem. 2017;43(3):905-914. doi:10.1159/000481640. Epub 2017 Sep 29. PubMed PMID: 28957796.

Liu J, Brown RE. Immunohistochemical detection of epithelial mesenchymal transition associated with stemness phenotype in anaplastic thyroid carcinoma. Int J Clin Exp Pathol. 2010 Oct 1;3(8):755-62. PubMed PMID: 21151388; PubMed Central PMCID: PMC2993225.

Li DD, Zhang YF, Xu HX, Zhang XP. The role of BRAF in the pathogenesis of thyroid carcinoma. Front Biosci (Landmark Ed). 2015 Jun 1;20:1068-78. Review. PubMed PMID: 25961545.

Lin SF, Lin JD, Chou TC, Huang YY, Wong RJ. Utility of a histone deacetylase inhibitor (PXD101) for thyroid cancer treatment. PLoS One. 2013 Oct 14;8(10):e77684. doi: 10.1371/journal.pone.0077684. eCollection 2013. PubMed PMID: 24155971; PubMed Central PMCID: PMC3796495.

Lu C, Stewart DJ, Lee JJ, Ji L, Ramesh R, Jayachandran G, Nunez MI, Wistuba II, Erasmus JJ, Hicks ME, Grimm EA, Reuben JM, Baladandayuthapani V, Templeton NS, McMannis JD, Roth JA. Phase I clinical trial of systemically administered TUSC2(FUS1)-nanoparticles mediating functional gene transfer in humans. PLoS One.2012;7(4):e34833. doi: 10.1371/journal.pone.0034833. Epub 2012 Apr 25. PubMed PMID: 22558101; PubMed Central PMCID: PMC3338819.

Liu R, Xing M. Diagnostic and prognostic TERT promoter mutations in thyroid fine-needle aspiration biopsy. Endocr Relat Cancer. 2014 Oct;21(5):825-30. doi:10.1530/ERC-14-0359. Epub 2014 Aug 13. PubMed PMID: 25121551; PubMed Central PMCID: PMC4175020.

Luzón-Toro B, Fernández RM, Villalba-Benito L, Torroglosa A, Antiñolo G, Borrego S. Influencers on Thyroid Cancer Onset: Molecular Genetic Basis. Genes (Basel). 2019 Nov 8;10(11). pii: E913. doi: 10.3390/genes10110913. Review. PubMed PMID: 31717449; PubMed Central PMCID: PMC6895808.

Martìn-Padura I, Lostaglio S, Schneemann M, Williams L, Romano M, Fruscella P,Panzeri C, Stoppacciaro A, Ruco L, Villa A, Simmons D, Dejana E. Junctional adhesion molecule, a novel member of the immunoglobulin superfamily that distributes at intercellular junctions and modulates monocyte transmigration. J Cell Biol. 1998 Jul 13;142(1):117-27. PubMed PMID: 9660867; PubMed Central PMCID:PMC2133024.

McSherry EA, McGee SF, Jirstrom K, Doyle EM, Brennan DJ, Landberg G, Dervan PA, Hopkins AM, Gallagher WM. JAM-A expression positively correlates with poor prognosis in breast cancer patients. Int J Cancer. 2009 Sep 15;125(6):1343-51.doi: 10.1002/ijc.24498. PubMed PMID: 19533747.

Melo M, da Rocha AG, Vinagre J, Sobrinho-Simões M, Soares P. Coexistence of TERT Promoter and BRAF Mutations in Papillary Thyroid Carcinoma: Added Value in Patient Prognosis? J Clin Oncol. 2015 Feb 20;33(6):667-8. doi: 10.1200/JCO.2014.59.4614. Epub 2015 Jan 20. PubMed PMID: 25605839.

Minna E, Romeo P, Dugo M, De Cecco L, Todoerti K, Pilotti S, Perrone F, Seregni E, Agnelli L, Neri A, Greco A, Borrello MG. miR-451a is underexpressed and targets AKT/mTOR pathway in papillary thyroid carcinoma. Oncotarget. 2016 Mar 15;7(11):12731-47. doi: 10.18632/oncotarget.7262. Review. Erratum in: Oncotarget. 2018 Feb 23;9(15):12534. PubMed PMID: 26871295; PubMed Central PMCID: PMC4914318.

Molinaro E, Romei C, Biagini A, Sabini E, Agate L, Mazzeo S, Materazzi G, Sellari-Franceschini S, Ribechini A, Torregrossa L, Basolo F, Vitti P, Elisei R. Anaplastic thyroid carcinoma: from clinicopathology to genetics and advanced therapies. Nat Rev Endocrinol. 2017 Nov;13(11):644-660. doi:10.1038/nrendo.2017.76. Epub 2017 Jul 14. Review. PubMed PMID: 28707679.

Montone KT, Baloch ZW, LiVolsi VA. The thyroid Hürthle (oncocytic) cell and its associated pathologic conditions: a surgical pathology and cytopathology review. Arch Pathol Lab Med. 2008

Aug;132(8):1241-50. doi:10.1043/1543-2165(2008)132[1241:TTHOCA]2.0.CO;2. Review. PubMed PMID: 18684023.

Morales I, Guzmán-Martínez L, Cerda-Troncoso C, Farías GA, Maccioni RB.Neuroinflammation in the pathogenesis of Alzheimer's disease. A rational framework for the search of novel therapeutic approaches. Front Cell Neurosci. 2014 Apr 22;8:112. doi: 10.3389/fncel.2014.00112. eCollection 2014. Review. PubMed PMID: 24795567; PubMed Central PMCID: PMC4001039.

Mulligan LM. RET revisited: expanding the oncogenic portfolio. Nat Rev Cancer.2014 Mar;14(3):173-86. doi: 10.1038/nrc3680. Review. PubMed PMID: 24561444.

Murugan AK, Xing M. Anaplastic thyroid cancers harbor novel oncogenic mutations of the ALK gene. Cancer Res 2011; 71:4403-4411 doi: 10.1158/0008-5472.CAN-10-4041

Naik MU, Naik TU, Suckow AT, Duncan MK, Naik UP. Attenuation of junctional adhesion molecule-A is a contributing factor for breast cancer cell invasion. Cancer Res. 2008 Apr 1;68(7):2194-203. doi: 10.1158/0008-5472.CAN-07-3057. PubMed PMID: 18381425.

Nucera C, Nehs MA, Nagarkatti SS, Sadow PM, Mekel M, Fischer AH, Lin PS, Bollag GE, Lawler J, Hodin RA, Parangi S. Targeting BRAFV600E with PLX4720 displays potent antimigratory and anti-invasive activity in preclinical models of human thyroid cancer. Oncologist. 2011;16(3):296-309. doi:10.1634/theoncologist.2010-0317. Epub 2011 Feb 25. PubMed PMID: 21355020; PubMed Central PMCID: PMC3073446.

Orlandella FM, Di Maro G, Ugolini C, Basolo F, Salvatore G.TWIST1/miR-584/TUSC2 pathway induces resistance to apoptosis in thyroid cancer cells. Oncotarget. 2016 Oct 25;7(43):70575-70588. doi: 10.18632/oncotarget.12129.PubMed PMID: 27661106; PubMed Central PMCID: PMC5342575.

Patel KN, Shaha AR. Poorly differentiated thyroid cancer. Curr Opin Otolaryngol Head Neck Surg. 2014 Apr;22(2):121-6. doi:10.1097/MOO.0000000000000037. Review. PubMed PMID: 24492853.

Penna-Martinez M, Epp F, Kahles H, Ramos-Lopez E, Hinsch N, Hansmann ML, Selkinski I, Grünwald F, Holzer K, Bechstein WO, Zeuzem S, Vorländer C, Badenhoop K. FOXE1 association with differentiated thyroid cancer and its progression. Thyroid. 2014 May;24(5):845-51. doi: 10.1089/thy.2013.0274. Epub 2014 Jan 29. PubMed PMID: 24325646; PubMed Central PMCID: PMC4026307.

Perri F, Pezzullo L, Chiofalo MG, Lastoria S, Di Gennaro F, Scarpati GD, Caponigro F. Targeted therapy: A new hope for thyroid carcinomas. Crit Rev Oncol Hematol. 2014 Nov 1. pii: S1040-8428(14)00172-3. doi: 10.1016/j.critrevonc.2014.10.012. Review. PubMed PMID: 25465739.

Pozdeyev N, Rose MM, Bowles DW, Schweppe RE. Molecular therapeutics for anaplastic thyroid cancer. Semin Cancer Biol. 2020 Apr;61:23-29. doi: 10.1016/j.semcancer.2020.01.005. Epub 2020 Jan 25. PubMed PMID: 31991166; PubMed Central PMCID: PMC7117889.

Prudkin L, Behrens C, Liu DD, Zhou X, Ozburn NC, Bekele BN, Minna JD, Moran C, Roth JA, Ji L, Wistuba II. Loss and reduction of FUS1 protein expression is a frequent phenomenon in the pathogenesis of lung cancer. Clin Cancer Res. 2008 Jan 1;14(1):41-7. doi: 10.1158/1078-0432.CCR-07-1252. PubMed PMID: 18172250; PubMed Central PMCID: PMC2833352.

Rebuffat SA, Kammoun-Krichen M, Charfeddine I, Ayadi H, Bougacha-Elleuch N, Peraldi-Roux S. IL-1β and TSH disturb thyroid epithelium integrity in autoimmune thyroid diseases. Immunobiology. 2013 Mar;218(3):285-91. doi:10.1016/j.imbio.2012.05.016. Epub 2012 Jun 23. PubMed PMID: 22878044.

Rimkus T, Sirkisoon S, Harrison A, Lo HW. Tumor suppressor candidate 2 (TUSC2,FUS-1) and human cancers. Discov Med. 2017 May;23(128):325-330. Review. PubMed PMID: 28715648; PubMed Central PMCID: PMC5808457.

Runkle EA, Mu D. Tight junction proteins: from barrier to tumorigenesis. Cancer Lett. 2013 Aug 28;337(1):41-8. doi: 10.1016/j.canlet.2013.05.038. Epub 2013 Jun 3. Review. PubMed PMID: 23743355; PubMed Central PMCID: PMC3752309.

Ruvolo PP. The broken "Off" switch in cancer signaling: PP2A as a regulator of tumorigenesis, drug resistance, and immune surveillance. BBA Clin. 2016 Aug 3;6:87-99. doi: 10.1016/j.bbacli.2016.08.002. eCollection 2016 Dec. Review. PubMed PMID: 27556014; PubMed Central PMCID: PMC4986044.

Santoro M, Dathan NA, Berlingieri MT, Bongarzone I, Paulin C, Grieco M, Pierotti MA, Vecchio G, Fusco A. Molecular characterization of RET/PTC3; a novel rearranged version of the RETproto-oncogene in a human thyroid papillary carcinoma. Oncogene. 1994 Feb;9(2):509-16. PubMed PMID: 8290261.

Sasanakietkul T, Murtha TD, Javid M, Korah R, Carling T. Epigenetic modifications in poorly differentiated and anaplastic thyroid cancer. Mol Cell Endocrinol. 2018 Jul 5;469:23-37. doi: 10.1016/j.mce.2017.05.022. Epub 2017 May 25. Review. PubMed PMID: 28552796.

Schrecengost RS, Green CL, Zhuang Y, Keller SN, Smith RA, Maines LW, Smith CD.In Vitro and In Vivo Antitumor and Anti-Inflammatory Capabilities of the Novel GSK3 and CDK9 Inhibitor ABC1183. J Pharmacol Exp Ther. 2018 Apr;365(1):107-116.doi: 10.1124/jpet.117.245738. Epub 2018 Feb 6. PubMed PMID: 29434052; PubMed Central PMCID: PMC5830635.

Siegel RL, Miller KD, Jemal A. Cancer Statistics, 2017. CA Cancer J Clin. 2017 Jan;67(1):7-30. doi: 10.3322/caac.21387. Epub 2017 Jan 5. PubMed PMID: 28055103.

Singh M, Yelle N, Venugopal C, Singh SK. EMT: Mechanisms and therapeutic implications. Pharmacol Ther. 2018 Feb;182:80-94. doi:10.1016/j.pharmthera.2017.08.009. Epub 2017 Aug 20. Review. PubMed PMID:28834698.

Smallridge RC. Approach to the patient with anaplastic thyroid carcinoma. J Clin Endocrinol Metab. 2012 Aug;97(8):2566-72. doi: 10.1210/jc.2012-1314. PubMed PMID: 22869844; PubMed Central PMCID: PMC3410281.

Smith N, Nucera C. Personalized therapy in patients with anaplastic thyroid cancer: targeting genetic and epigenetic alterations. J Clin Endocrinol Metab.2015 Jan;100(1):35-42. doi: 10.1210/jc.2014-2803. PubMed PMID: 25347569; PubMed Central PMCID: PMC4283016.

Songyang Z, Fanning AS, Fu C, Xu J, Marfatia SM, Chishti AH, Crompton A, Chan AC, Anderson JM, Cantley LC. Recognition of unique carboxyl-terminal motifs by distinct PDZ domains. Science. 1997 Jan 3;275(5296):73-7. PubMed PMID: 8974395.

Steinbacher T, Kummer D, Ebnet K. Junctional adhesion molecule-A: functional diversity through molecular promiscuity. Cell Mol Life Sci. 2018 Apr;75(8):1393-1409. doi: 10.1007/s00018-017-2729-0. Epub 2017 Dec 14. Review. PubMed PMID: 29238845.

Sun W, Xu Y, Zhao C, Hao F, Chen D, Guan J, Zhang K. Targeting TGF-β1suppresses survival of and invasion by anaplastic thyroid carcinoma cells. Am J Transl Res. 2017 Mar 15;9(3):1418-1425. eCollection 2017. PubMed PMID: 28386367; PubMed Central PMCID: PMC5376032.

Tarulli GA, Stanton PG, Loveland KL, Rajpert-De Meyts E, McLachlan RI, Meachem SJ. A survey of Sertoli cell differentiation in men after gonadotropin suppression and in testicular cancer. Spermatogenesis. 2013 Jan 1;3(1):e24014.PubMed PMID: 23687617; PubMed Central PMCID: PMC3644048.

Thawani JP, Wang AC, Than KD, Lin CY, La Marca F, Park P. Bone morphogenetic proteins and cancer: review of the literature. Neurosurgery. 2010 Feb;66(2):233-46; discussion 246. doi: 10.1227/01.NEU.0000363722.42097.C2.Review. PubMed PMID: 20042986.

Tiedje V, Stuschke M, Weber F, Dralle H, Moss L, Führer D. Anaplastic thyroid carcinoma: review of treatment protocols. Endocr Relat Cancer. 2018 Mar;25(3):R153-R161. doi: 10.1530/ERC-17-0435. Epub 2018 Jan 2. Review. PubMed PMID: 29295821.

Uno F, Sasaki J, Nishizaki M, Carboni G, Xu K, Atkinson EN, Kondo M, Minna JD, Roth JA, Ji L. Myristoylation of the fus1 protein is required for tumor suppression in human lung cancer cells. Cancer Res. 2004 May 1;64(9):2969-76.PubMed PMID: 15126327.

Wang Y, Lui WY. Transforming growth factor-β1 attenuates junctional adhesion molecule-A and contributes to breast cancer cell invasion. Eur J Cancer. 2012 Dec;48(18):3475-87. doi: 10.1016/j.ejca.2012.04.016. Epub 2012 May 28. PubMed PMID: 22647687.

Wiseman SM, Griffith OL, Deen S, Rajput A, Masoudi H, Gilks B, Goldstein L,Gown A, Jones SJ. Identification of molecular markers altered during transformation of differentiated into anaplastic thyroid carcinoma. Arch Surg. 2007 Aug;142(8):717-27; discussion 727-9. PubMed PMID: 17709725.

Xie H.H., Huan W.T., Han J.Q., Ren W.R., Yang L.H. MicroRNA-663 facilitates the growth, migration and invasion of ovarian cancer cell by inhibiting TUSC2. Biological Research, 03 Apr 2019, 52(1):18 DOI: 10.1186/s40659-019-0219-6 PMID: 30944041 PMCID: PMC6448305

Xin J, Zhang XK, Xin DY, Li XF, Sun DK, Ma YY, Tian LQ. FUS1 acts as a tumor-suppressor gene by upregulating miR-197 in human glioblastoma. Oncol Rep. 2015 Aug;34(2):868-76. doi: 10.3892/or.2015.4069. Epub 2015 Jun 16. PubMed PMID: 26081814.

Xiaobo C, Majidi M, Feng M, Shao R, Wang J, Zhao Y, Baladandayuthapani V, Song J, Fang B, Ji L, Mehran R, Roth JA. TUSC2(FUS1)-erlotinib Induced Vulnerabilities in Epidermal Growth Factor Receptor(EGFR) Wildtype Non-small Cell Lung Cancer(NSCLC) Targeted by the Repurposed Drug Auranofin. Sci Rep. 2016 Nov15;6:35741. doi: 10.1038/srep35741. PubMed PMID: 27845352; PubMed Central PMCID:PMC5109231.

Xing M. Molecular pathogenesis and mechanisms of thyroid cancer. Nat Rev Cancer. 2013 Mar;13(3):184-99. doi: 10.1038/nrc3431. Review. PubMed PMID:23429735; PubMed Central PMCID: PMC3791171.

Xin J, Zhang XK, Xin DY, Li XF, Sun DK, Ma YY, Tian LQ. FUS1 acts as a tumor-suppressor gene by upregulating miR-197 in human glioblastoma. Oncol Rep. 2015 Aug;34(2):868-76. doi: 10.3892/or.2015.4069. Epub 2015 Jun 16. PubMed PMID: 26081814.

Xu B, Ghossein R. Genomic Landscape of poorly Differentiated and Anaplastic Thyroid Carcinoma. Endocr Pathol. 2016 Sep;27(3):205-12. doi:10.1007/s12022-016-9445-4. Review. PubMed PMID: 27372303.

Yazlovitskaya EM, Voziyan PA, Manavalan T, Yarbrough WG, Ivanova AV. Cellular oxidative stress response mediates radiosensitivity in Fus1-deficient mice. Cell Death Dis. 2015 Feb 19;6:e1652. doi: 10.1038/cddis.2014.593. PubMed PMID:25695605; PubMed Central PMCID: PMC4669799.

Zhang M, Luo W, Huang B, Liu Z, Sun L, Zhang Q, Qiu X, Xu K, Wang E. Overexpression of JAM-A in non-small cell lung cancer correlates with tumor progression. PLoS One. 2013 Nov 12;8(11):e79173. doi:10.1371/journal.pone.0079173. eCollection 2013. PubMed PMID: 24265754; PubMed Central PMCID: PMC3827132.

Zhang B, Xu X, Qi Z, Peng L, Qiu B, Huo X. The FUS1 gene inhibits EC109 cell growth mediated by a lentivirus vector. Br J Biomed Sci. 2013;70(1):22-6. PubMed PMID: 23617094.